$Ca^{40}(d,p)Ca^{41}$, a Test of the Validity of the Distorted-Wave Born Approximation*

L. L. Lee, Jr., J. P. Schiffer, and B. Zeidman
Argonne National Laboratory, Argonne, Illinois

and

G. R. Satchler, R. M. Drisko, and R. H. Bassel
Oak Ridge National Laboratory, Oak Ridge, Tennessee

(Received 6 July 1964)

The reaction $Ca^{40}(d,p)Ca^{41}$ has been studied at deuteron energies of 7.0, 8.0, 9.0, 10.0, 11.0, and 12.0 MeV. Absolute differential cross sections for the four most prominent proton groups were measured and are compared with predictions based on the distorted-wave Born approximation (DWBA). Particular emphasis is placed on the ability of this approach to extract precise spectroscopic factors, which for this reaction are expected to be known *a priori*. Effects of variation of optical parameters, and of inclusion of spin-orbit and finite-range effects, are discussed in detail. It can be concluded that, if one uses optical potentials which fit elastic-scattering data, spectroscopic factors can be extracted with an accuracy of 20% or better.

I. INTRODUCTION

DEUTERON-STRIPPING reactions have been a valuable tool of nuclear spectroscopy for more than a decade. The simple plane-wave theory, as formulated first by Butler,[1] showed that a measurement of the proton angular distribution from a (d,p) reaction[2] could, in favorable cases, determine the orbital angular momentum transferred to the residual nucleus. This immediately indicates the parity change in the reaction, and often provides useful restrictions on the spin of the final state. In the particular case of a zero-spin target, the spin is determined to within one unit.

Additional nuclear-structure information can be obtained from the intensities of the observed proton groups. The (d,p) reaction is highly selective, strongly populating only those states in the residual nucleus that can be obtained by simply adding a neutron to the ground state of the target nucleus. Several single-particle orbitals may be available for the captured neutron, and the degree to which a residual state satisfies this condition for a particular single-particle orbital (l,j) is called its spectroscopic factor $S(l,j)$ for that orbital. The $S(l,j)$ is unity if the state exhausts the single-particle strength, as would occur in capture by a closed-shell nucleus into a pure single-particle state. The use of spectroscopic factors (or "reduced widths") to obtain nuclear-structure information has been discussed in considerable detail by Macfarlane and French.[3]

The early plane-wave stripping theory was remarkably successful as a tool for identifying l values from measured (d,p) angular distributions from light nuclei, and even gave good fits to the shape of the main peak in the angular distribution. However, it was quickly noted[4] that the predicted absolute cross sections were frequently too large by an order of magnitude or more. Thus, absolute values of spectroscopic factors could not be obtained, and semiempirical methods based on relative cross sections had to be devised.[3] However, the failure to predict absolute cross sections also cast some doubt on the ability of the plane-wave theory to give a correct account of relative cross sections and their dependence on energy and Q value. As experimental data for heavier nuclei became available, it became clear that the angular distributions also deviated considerably from the expectations of the simple theory, and that at the very least, distortion due to the Coulomb field was important. We now know that distortion by nuclear scattering and absorption is always important. In fact, under no circumstances met with experimentally are distortion effects negligible, so a plane-wave theory is *never* a good approximation.

It was proposed that the interaction could be more accurately described by the distorted-wave (DW) Born approximation.[5,6] The DW theory takes account of the scattering and absorption of the incident deuteron before stripping, and of the emergent proton, by replacing the plane waves by distorted or elastic-scattering waves. In practice, these are generated by optical-model potentials that reproduce the observed elastic scattering

* Work performed under the auspices of the U. S. Atomic Energy Commission.

[1] S. T. Butler and O. H. Hittmair, *Nuclear Stripping Reactions* (John Wiley & Sons Inc., New York, 1959).

[2] For simplicity, the present discussion is in terms of the (d,p) reaction, but applies equally well to (d,n) reactions, and of course, to the inverse pickup reactions.

[3] M. H. Macfarlane and J. B. French, Rev. Mod. Phys. **32**, 567 (1960); J. B. French, in *Nuclear Spectroscopy*, edited by F. Ajzenberg-Selove (Academic Press Inc., New York, 1960), Part B.

[4] Y. Fujimoto, *Proceedings of the International Conference of Theoretical Physics* (Universities of Kyoto and Tokyo, 1953).

[5] J. Horowitz and A. M. L. Messiah, J. Phys. Radium **14**, 695, 731 (1953); W. Tobocman, Phys. Rev. **94**, 1655 (1954).

[6] W. Tobocman, *Theory of Direct Nuclear Reactions* (Oxford University Press, New York, 1961); N. Austern, *Fast Neutron Physics*, edited by J. B. Marion and J. L. Fowler (Interscience Publishers, Inc., New York, 1963), Vol. II; R. Huby, M. Y. Rafai, and G. R. Satchler, Nucl. Phys. **9**, 94 (1958); G. R. Satchler and W. Tobocman, Phys. Rev. **118**, 1566 (1960); L. C. Biedenharn and G. R. Satchler, Helv. Phys. Acta, Suppl. **6**, 372 (1960); G. R. Satchler, Nucl. Phys. **18**, 110 (1960); L. J. B. Goldfarb and R. C. Johnson, *ibid.* **18**, 353 (1960); **21**, 462 (1960); B. Buck and P. E. Hodgson, Phil. Mag. **6**, 1371 (1961); D. Robson, Nucl. Phys. **22**, 34, 47 (1961); R. C. Johnson, *ibid.* **35**, 654 (1962); R. H. Bassel, R. M. Drisko, and G. R. Satchler, Oak Ridge National Laboratory Report ORNL-3240 (unpublished).

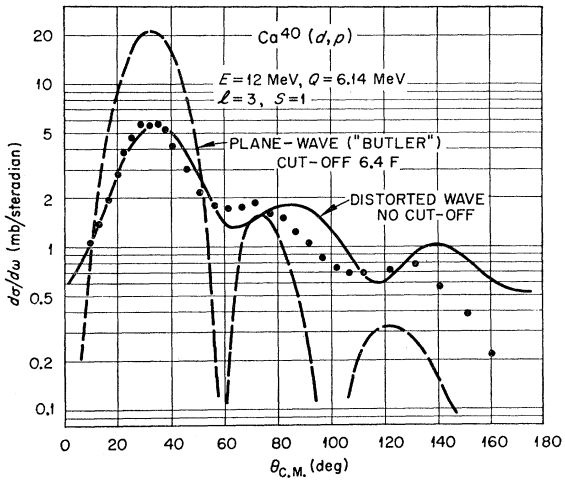

FIG. 1. Comparison of plane-wave and distorted-wave predictions for $Ca^{40}(d,p)$ ground-state transition. A type-Z deuteron potential was used. The plane-wave cutoff was chosen to give the correct position for the main peak.

from the same nucleus at the same energy, and whose parameters are thereby determined. Considerable effort has gone into the exploitation of this theory,[6] and the numerous comparisons[7–9] with experimental data suggest that quantitatively accurate predictions are possible.

In Fig. 1, a distorted-wave and a plane-wave calculation are compared with experimental results for the $Ca^{40}(d,p)$ ground-state transition at 12 MeV. Both calculations use the same wave function for the captured neutron and assume a spectroscopic factor of unity. This figure emphasizes how the plane-wave version predicts quite wrong magnitudes for the (d,p) reaction and gives a very poor account of the angular distribution, whereas the distorted-wave theory is very much better. The present paper reports an attempt to make a more detailed test of the validity of the latter theory.

Most previous DW analyses of (d,p) data were made for nuclei for which no accurate estimate of the spectroscopic factors could be made *a priori*. In addition, in many cases elastic-scattering data were not available, so that the parameters of the optical potential were often treated as adjustable. Indeed, only recently have detailed analyses of deuteron elastic scattering become available.[10] Consequently, the theory was only tested qualitatively. There are a few notable exceptions[8,9] in which attempts were made, similar to the one reported here, to obtain and analyze both elastic-scattering and stripping-reaction data. In no case, however, could the spectroscopic factor be predicted definitely. It is worth noting that one of these analyses,[9] the one for $Pb^{206}(d,p)$, led to the tentative conclusion that the deuteron optical parameters that were needed to fit the (d,p) angular distributions would not successfully reproduce the observed elastic scattering. This inadequacy was taken as indicating a partial failure of the simple theory.

The present work emphasizes two aspects of the comparison between experiment and theory. One is to make a detailed test of the theory. For this purpose, all relevant features that can be handled at the present time, such as spin-orbit coupling and the finite range of the neutron-proton interaction, are taken into consideration. On the other hand, an attempt is made to gauge the success of the simplified zero-range theory without spin-orbit coupling, since numerous groups have access to computer codes based on this version of the theory. At the same time, simple prescriptions are suggested by which the spectroscopic factors so obtained can be approximately corrected for the neglected effects.

The reaction $Ca^{40}(d,p)Ca^{41}$ was chosen for this study because Ca^{40} is believed to be well described as a closed-shell nucleus. The final states in Ca^{41} are therefore believed to correspond to the addition of a single neutron to an inert and spherical Ca^{40} core, so that the spectroscopic factors are predicted to be unity. This allows a more rigorous test of the ability of the DW theory considered here to give correct absolute cross sections. Moreover, Ca^{40} is heavy enough that the common difficulties encountered in work with very light nuclei are not expected to be so important. Further, the measurements were made over the range of deuteron energies from 7 to 12 MeV in order to observe the effect of changing the incident deuteron energy.

The elastic scattering of deuterons from Ca^{40} was also measured at the same energies; the results together with optical-model analyses are published in the preceding paper.[11] Unfortunately, the elastic scattering of protons from Ca^{41} cannot be measured. However, the systematics of the parameters of the optical potential for proton scattering are probably known sufficiently well[12] to make this disadvantage a minor one. In

[7] W. Tobocman, Phys. Rev. **115**, 99 (1959); W. Tobocman and W. R. Gibbs, *ibid.* **126**, 1076 (1962); W. R. Smith and E. Ivash, *ibid.* **128**, 1175 (1962); **131**, 304 (1963); B. Buck and P. E. Hodgson, Nucl. Phys. **29**, 496 (1962); H. D. Scott, *ibid.* **27**, 490 (1962); P. Mukherjee and B. L. Cohen, Phys. Rev. **127**, 1284 (1962); K. Ilakovac, L. G. Kuo, M. Petravic, I. Slaus, P. Tomas, and G. R. Satchler, *ibid.* **128**, 2739 (1962); C. D. Goodman, J. B. Ball, and C. B. Fulmer, *ibid.* **127**, 574 (1962); C. Daum, Nucl. Phys. **45**, 273 (1963); B. L. Cohen and O. V. Chubinsky, Phys. Rev. **131**, 2184 (1963); E. K. Lin and B. L. Cohen, *ibid.* **132**, 2632 (1963); J. L. Yntema, *ibid.* **131**, 811 (1963); M. N. Vergnes and R. K. Sheline, *ibid.* **132**, 1736 (1963); J. Testoni, S. Mayo, and P. E. Hodgson, Nucl. Phys. **50**, 479 (1964). See also H. E. Gove, in *Proceedings of the Rutherford Jubilee International Conference, Manchester, 1961*, edited by J. B. Birks (Heywood and Company, Ltd., London, 1962), and other work referred to there.

[8] S. Hinds, R. Middleton, and D. J. Pullen, Phys. Letters **1**, 12 (1962); B. E. F. Macefield, R. Middleton, and D. J. Pullen, Nucl. Phys. **44**, 309 (1963); P. T. Andrews, R. W. Clifft, L. L. Green, and J. F. Sharpey-Schafer (to be published).

[9] D. W. Miller, H. E. Wegner, and W. S. Hall, Phys. Rev. **125**, 2054 (1962).

[10] C. M. Perey and F. G. Perey, Phys. Rev. **132**, 755 (1963); E. C. Halbert, Nucl. Phys. **50**, 353 (1964).

[11] R. H. Bassel, R. M. Drisko, G. R. Satchler, L. L. Lee, Jr., J. P. Schiffer, and B. Zeidman, Phys. Rev. **136**, B960 (1964), preceding paper.

[12] F. G. Perey, Phys. Rev. **131**, 745 (1963).

addition, the considerable amount of available information on the scattering of 8–14-MeV protons on Ar^{40} has been analyzed,[13] and the results have been used in the present work. The potential required is consistent with that extrapolated from other nuclei.[12] Moreover, the scattering of 12-MeV protons on Ca^{42}, reported[14] since the analysis was completed, was well fitted by the same potential (see Fig. 9 below). In any case, as will be shown below, the (d,p) predictions are rather insensitive to small uncertainties in the proton parameters.

II. THEORY

Before proceeding with the analysis, we should review briefly the DW theory as used here, indicating its limitations and the extent to which we may expect it to apply. The theory for the $A(d,p)B$ reaction is based upon a transition amplitude of the form

$$T=\int\int \chi_p^{(-)}(\mathbf{k}_p,\mathbf{r}_p)^*\langle B|V|A\rangle\chi_d^{(+)}(\mathbf{k}_d,\mathbf{r}_d)d\mathbf{r}_p d\mathbf{r}_d. \quad (1)$$

The $\chi(k,r)$ are distorted waves for the scattering of a pair of particles with relative momentum $\mathbf{k}$ and separation $\mathbf{r}$. The other factor in the integrand is the matrix element of the interaction integrated over all the coordinates independent of $\mathbf{r}_p$ and $\mathbf{r}_d$. The details of the evaluation of the amplitude (1) have been described in many places.[5,6,15]

Approximate amplitudes of the form (1) may be derived in a number of ways.[5,6,16] In particular, a commonly used derivation gives the final-state interaction potential

$$V=V_{pB}-U_{pB},$$

where U_{pB} is the optical potential used to generate χ_p. If the nucleus B is formed by target A stripping a neutron from the deuteron, then we may write

$$V=V_{pn}+(V_{pA}-U_{pB}). \quad (2)$$

It is usually argued that the term V_{pn} dominates, and this seems physically reasonable [especially if one considers the inverse (p,d) pickup reaction]. Clearly, there is considerable cancellation between V_{pA} and U_{pB}, but this can never be complete for finite nuclei. For one thing, V_{pA} has off-diagonal matrix elements which allow A to be excited. Further, if U_{pB} is chosen to reproduce the observed scattering of p on B, it contains an appreciable imaginary part, but V_{pA} is real if it represents the elementary interaction of p with A. On the other hand, V_{pA} may represent an effective (and complex) interaction in the sense of Watson and Brueckner; or somewhat equivalently, we may argue that higher order effects will tend to cancel those parts of U_{pB} not canceled by V_{pA}.

Additional complication arises through antisymmetrization; the emerging proton may have originated from the target nucleus A rather than from the stripped deuteron. This gives two possible processes, arising from the analog of the separation made in Eq. (2). One is knockout of a target proton by the incident deuteron, and the other is heavy-particle stripping in which the target nucleus is stripped rather than the deuteron. It is usually argued that these processes are less important because of the more complicated nuclear overlaps involved.

It is inappropriate here to discuss the relative merits of the various forms of the theory, or the importance of the various interaction terms. Rather, we take the view that we are testing the validity of the amplitude obtained by using $V=V_{pn}$ in Eq. (1), where V_{pn} is the true interaction between a free neutron and proton. We may regard this as an intuitive model to be tested against experiment. The preceding discussion is then intended to emphasize the possible shortcomings of such a model.

Now the interaction V_{pn} is not well known in detail; for example, it probably contains a hard core. Fortunately, it occurs as a product with ϕ_d, the internal wave function for the deuteron ground state, and we only need to know very simple properties of this product.[6] If we use the zero-range approximation we only need a normalization constant, because then we write

$$V_{np}\phi_d(r_{np})\equiv D(r_{np})\approx D_0\delta(r_{np}). \quad (3)$$

(This expression necessarily neglects the tensor force and D state, so that ϕ_d refers to the spatial part of the wave function only, and V_{np} is the triplet part of the interaction.) Equation (3) results immediately if V_{np} itself is of zero range, so that

$$\phi_d(s)=(\alpha/\pi)^{1/2}(\exp-\alpha s)/s, \quad (4)$$

where $\epsilon=\alpha^2\hbar^2/M$ is the deuteron binding energy. We then find

$$D_0^2=8\pi\epsilon^2/\alpha^3\approx 10^4\ \mathrm{MeV^2\ F^3}. \quad (5)$$

However, it is not necessary to make such a drastic approximation. Recognizing that D_0 is the value of the Fourier transform of D for zero momentum, we see that it depends only on the asymptotic normalization of ϕ_d for *large* separations r_{np}. Effective-range theory then leads[6] to the value

$$D_0^2\approx 1.5\times 10^4\mathrm{MeV^2F^3}. \quad (6)$$

(The same result is obtained by using the Hulthén form for ϕ_d.)

A more complete calculation uses a "finite-range" function for D instead of the approximation (3). In

[13] G. R. Satchler (to be published).
[14] A. Marinov, L. L. Lee, Jr., and J. P. Schiffer, Bull. Am. Phys. Soc. **9**, 457 (1964).
[15] G. R. Satchler, Nucl. Phys. **55**, 1 (1964).
[16] T. Wu and T. Ohmura, *Quantum Theory of Scattering* (Prentice-Hall, Inc., Englewood Cliffs, New Jersey, 1962); E. Gerjuoy, Ann. Phys. (N.Y.) **5**, 58 (1958); M. Gell-Mann and M. L. Goldberger, Phys. Rev. **91**, 398 (1953); N. C. Francis and K. M. Watson, *ibid.* **93**, 313 (1954); K. R. Greider, *ibid.* **133**, B1483 (1964).

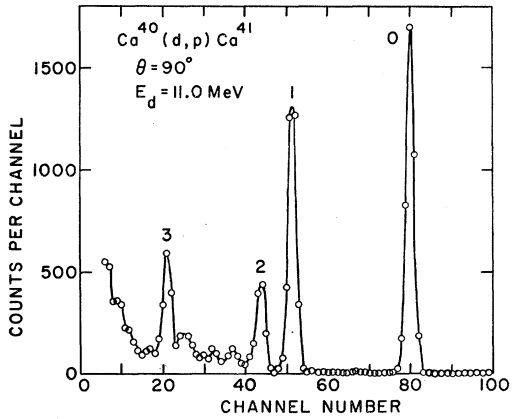

FIG. 2. Typical proton spectrum taken at 90° and 11.0-MeV deuteron energy. Peaks numbered 0–3 correspond to the ground state (Q=6.14 MeV), first excited state (Q=4.19 MeV), 2.47 excited state (Q=3.67 MeV), and the 3.95-MeV excited state (Q=2.19 MeV), respectively. The zero of energy has been suppressed to eliminate elastically scattered deuterons.

situations in which the zero-range approximation is reasonably good, so that finite-range corrections are not too large, the exact form of D is not important. If we use any function adjusted to have the same zero and small momentum components, we shall obtain reasonably accurate results. The calculations reported here use a Gaussian form

$$D(s)=D_G e^{-(s/R_G)^2}, \tag{7}$$

with R_G=1.25 F, D_G^2=127 MeV^{2}F^{-3}. Calculations with a Yukawa form for D, adjusted to have the same Fourier transform to order k^2, give almost identical results. An account of the theoretical implications of relaxing the zero-range approximation has been given elsewhere.[17]

A fundamental objection to the amplitude (1) may be raised against the use of a deuteron distorted wave that depends only on the position of the center of mass of the deuteron. Outside the nucleus this form is correct (except for the rather weak polarization by the Coulomb field), but one may expect the deuteron to suffer considerable internal distortion as it crosses the nuclear surface. Much of this distortion leads to breakup, and the consequent absorption into other channels is described in an average way by the imaginary part of the optical potential. Nonetheless, a fraction of these deuterons may contribute to the stripping amplitude even though they do not survive to contribute to the elastic wave. The usual optical-model potential, which depends only on the position of the center of mass of the deuteron, does not take explicit account of these possibilities, and hence the corresponding wave function is incorrect to that extent inside the nucleus. It has been argued[18] that this deficiency would be accounted for by completely neglecting contributions to the amplitude (1) from the nuclear interior, by using a cutoff on the stripping radial integrals. Unfortunately, the importance of these effects has not been estimated, so the validity of using a cutoff of this type can only be tested against experiment.

Another feature affecting the contributions from the nuclear interior arises from the possible nonlocality of the optical potentials. The observed energy dependence of the parameters required to fit elastic-scattering data may be interpreted as due to the nonlocality of the potential.[19] However, while a local and a nonlocal potential may be found to generate the same *asymptotic* wave functions (that is, give the same scattering), it is found[20] that the magnitude of the wave function in the nuclear interior is smaller for the nonlocal potential than for the local. (For low-energy nucleons this reduction is typically of the order of 15%.) Since this result is also true for the bound-state wave function for the captured neutron, the contributions from the nuclear interior to the amplitude (1) that result from the use of nonlocal potentials would be considerably smaller than those from the use of local potentials as in the calculations reported here.

Finally, a remark should be made concerning the various higher order effects which we lump together and call "compound-nucleus" processes. The only theoretical procedures available are based upon one form or another of the statistical model. In addition, the large number of open channels available in the present reaction (mostly to nuclear states of unknown spin) make accurate calculation with a model difficult. However, some estimates of compound-nucleus contributions have been made. The results of these are reported below, and details will be given elsewhere.[21]

III. EXPERIMENTAL MEASUREMENTS AND RESULTS

The absolute differential cross sections of the reaction $Ca^{40}(d,p)Ca^{41}$ were measured with the beam from the Argonne tandem Van de Graaff at incident-deuteron energies of 7.0, 8.0, 9.0, 10.0, 11.0, and 12.0 MeV, and at angles between 10 and 165°. The experimental equipment was the same as that described in the preceding paper[11] except that Li-drifted Si junction counters were used to detect the reaction protons. A typical spectrum at E_d=11.0 MeV and θ=90° is shown in Fig. 2; the energy resolution width was about 130 keV, and was determined principally by the target thickness. Difficulties were encountered at the extreme forward

[17] N. Austern, R. M. Drisko, E. C. Halbert, and G. R. Satchler, Phys. Rev. **133**, B3 (1964).

[18] G. R. Satchler, in *Proceedings of the Conference on Direct Interactions and Nuclear Reaction Mechanisms, Padua, 1962*, edited by E. Clementel and C. Villi (Gordon and Breach Science Publishers, Inc., New York, 1963).

[19] F. Perey and B. Buck, Nucl. Phys. **32**, 353 (1962).

[20] F. Perey, in *Proceedings of the Conference on Direct Interactions and Nuclear Reaction Mechanisms, Padua, 1962*, edited by E. Clementel and C. Villi (Gordon and Breach Science Publishers, Inc., New York, 1963).

[21] H. F. Bowsher, Bull. Am. Phys. Soc. **9**, 74 (1964); H. F. Bowsher and R. H. Bassel (to be published).

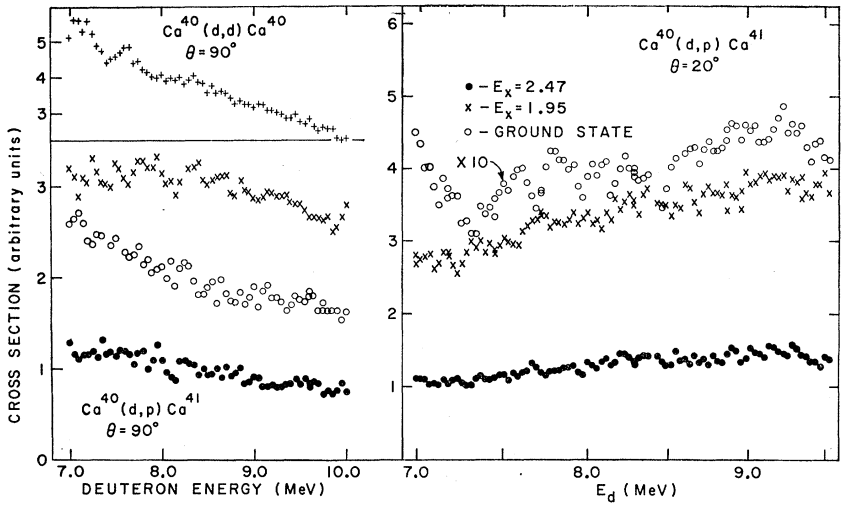

FIG. 3. Excitation curves at 20 and 90° for the reaction $Ca^{40}(d,p)Ca^{41}$ over the deuteron energy range from 7.0 to 10.0 MeV. While statistical errors are about twice the size of the points or less, there are probably greater uncertainties due to target nonuniformities as discussed in the text. The target was about 120-keV thick to the incident deuterons. A 90° excitation for elastic deuteron scattering by Ca is included for comparison.

angles ($\theta \leqslant 25°$) because of the large number of elastically scattered deuterons. Even when the beam was reduced sufficiently to eliminate pileup in the electronics, a considerable background was introduced from reactions of the elastically scattered deuterons in the Si detectors. It was therefore necessary to use gold absorbers in front of the counters at the extreme forward angles. These absorbers completely stopped the deuterons and appreciably increased the energy spread of the proton groups. It was still possible, however, to fully resolve the prominent groups of interest.

The pulse-height spectra were analyzed with a computer program, written by Taraba of the ANL Applied Mathematics Division, which summed the counts under specified peaks, subtracted background, and converted the yield into center-of-mass cross sections. The program also shifted the regions to be summed from one angle to the next in accordance with the kinematics of the reaction. The computer output also included plotted spectra, with and without background subtraction, and statistical errors in the final differential cross sections.

The reaction $Ca^{40}(d,p)Ca^{41}$ has been studied with high resolution by Bockelman and Buechner[22] and, more recently, by Belote *et al.*[23] These workers found that four final states below 4-MeV excitation in Ca^{41} are strongly populated, namely the ground state with an $l=3$ angular distribution and states at 1.95-, 2.47-, and 3.95-MeV excitation, all with $l=1$ angular distributions. These groups are indicated in the spectrum shown in Fig. 2. In the present experiment, angular distributions for these four proton groups were extracted from the data. In addition to statistical errors in the cross sections, small errors in the measurement of beam charge and target thickness were considered, as discussed in the preceding paper.[11] In addition, small errors are introduced at the extreme forward angles because of the difficulties discussed above.

The limited resolution of the present experiment also introduced some further uncertainties. The protons leading to the 1.95-MeV state were not resolved from those leading to the very weak level at 2.01-MeV excitation. However, the uncertainties so introduced are small compared with others discussed above. The yield attributed to the 3.95-MeV excited state also contains contributions from the states at 3.92- and 3.98-MeV excitation. At a deuteron energy of 7 MeV, the angular distributions for both of these groups are roughly isotropic, and their cross sections are about 1/30 of the peak cross section for the 3.95-MeV state.[23] If one assumes that the reaction to these two states proceeds through the compound nucleus, then these cross sections may be expected to decrease with increasing deuteron energy. Contributions from these states add a constant term to the cross section for the 3.95-MeV state which may be quite significant at back angles. The effect may be regarded as roughly equivalent to an increase in the compound-nucleus cross section for the 3.95-MeV state. It may be significant in filling in minima at backward angles, but will not alter the qualitative shape of the angular distribution or the spectroscopic factor determined from the forward maximum.

In order to determine whether or not the (d,p) cross sections varied smoothly with deuteron energy, excitation functions were measured at 90° (where compound-nucleus contributions are expected to be relatively large) and at 20° (near the forward stripping peaks). These excitation functions are shown in Fig. 3 along with a 90° excitation function for elastic deuteron scattering from Ca. It is evident that, at both angles, the plot of yield versus energy shows small fluctuations of up to 15%, and that these tend to damp out with increasing deuteron energy.

[22] C. K. Bockelman and W. W. Buechner, Phys. Rev. **107**, 1366 (1957).

[23] T. A. Belote, J. Rappoport, and W. W. Buechner, Bull. Am. Phys. Soc. **9**, 79 (1964); T. A. Belote (private communication).

TABLE I. Absolute differential cross sections in mb/sr for the reaction $Ca^{40}(d,p)Ca^{41}$ for the four prominent proton groups having the Q values indicated.[a]

E_d (MeV)	$\theta_{c.m.}$	$\sigma(\theta)$ $Q=6.14$ MeV	4.19 MeV	3.67 MeV	2.19 MeV
7.0	11.3	1.48	11.1	4.13	10.2
	15.4	1.84	14.4	5.64	12.8
	20.5	2.10	16.0	6.21	12.1
	25.6	2.48	13.1	5.11	10.5
	30.8	3.06	8.57	3.34	6.79
	35.9	3.23	5.34	2.19	4.24
	41.0	3.41	3.80	1.48	2.53
	46.1	3.13	3.63	1.36	2.66
	51.2	2.76	4.15	1.52	4.10
	56.4	2.24	4.28	1.51	4.35
	61.4	1.70	4.18	1.56	4.40
	66.5	1.47	3.51	1.42	4.13
	71.5	1.33	2.74	1.21	3.53
	76.5	1.31	2.25	0.992	2.99
	81.6	1.41	1.72	0.809	2.34
	86.6	1.47	1.32	0.586	1.66
	91.6	1.60	1.30	0.490	1.17
	96.6	1.60	1.18	0.413	0.761
	101.6	1.47	1.13	0.357	0.761
	106.5	1.35	0.995	0.214	0.543
	111.5	1.25	0.995	0.264	0.380
	116.4	1.11	0.871	0.245	0.543
	126.3	0.922	0.820	0.289	
	131.2	0.849	0.741	0.308	
	136.1	0.741	0.719	0.270	
	141.0	0.770	0.820	0.315	
	145.8	0.733	0.806	0.292	
	150.8	0.791	0.828	0.284	
	155.7	0.661	0.900	0.259	
	160.5	0.581	0.958	0.315	
	165.4	0.559	1.02	0.280	
	168.3	0.552	1.02	0.306	
8.0	11.3	1.66	21.8	7.21	18.3
	15.4	1.96	25.9	8.29	19.8
	20.5	2.40	25.6	8.60	20.6
	25.6	2.94	17.7	5.99	14.3
	30.8	3.86	10.5	3.74	8.02
	35.9	4.34	5.94	2.20	5.26
	41.0	4.37	4.76	1.73	3.92
	46.1	3.81	5.33	1.98	4.33
	51.2	3.33	5.80	2.01	4.67
	56.3	2.41	5.01	1.81	4.67
	61.3	1.96	4.31	1.75	4.02
	66.4	1.92	3.34	1.17	3.35
	71.4	1.73	2.34	0.957	2.63
	76.5	1.83	1.84	0.810	2.42
	81.5	1.87	1.55	0.687	1.84
	86.5	1.87	1.55	0.724	1.27
	91.6	1.70	1.59	0.564	1.32
	96.5	1.61	1.56	0.546	1.08
	101.5	1.52	1.42	0.410	1.08
	106.5	1.49	1.36	0.44	1.12
	111.4	1.28	1.16	0.28	1.17
	116.4	1.36	1.08	0.32	1.39
	121.3	1.19	0.886	0.31	1.60
	126.3	1.15	0.904	0.31	1.99
	131.2	1.07	0.877	0.31	1.96
	136.1	0.99	0.913	0.29	2.03
	141.0	0.827	0.931	0.40	2.03
	145.9	0.808	1.02	0.37	1.53
	150.8	0.827	1.01	0.31	1.36
	155.6	0.751	0.913	0.37	0.93
	160.5	0.685	0.877	0.24	1.01
	165.4	0.571	1.003	0.31	0.86
	168.3	0.637	1.12	0.36	1.05
9.0	11.3	1.52	21.1	10.1	14.6
	15.4	2.08	28.6	12.5	17.5
	20.6	2.44	26.5	10.9	14.5

E_d (MeV)	$\theta_{c.m.}$	$\sigma(\theta)$ $Q=6.14$ MeV	4.19 MeV	3.67 MeV	2.19 MeV
9.0	25.7	3.23	18.4	6.98	8.76
	30.8	3.90	9.58	3.98	5.68
	35.9	4.54	5.36	2.34	3.08
	41.0	5.43	5.10	2.31	2.85
	46.2	3.85	5.77	2.39	3.02
	51.2	2.82	6.07	2.47	3.37
	56.3	2.34	5.36	2.11	3.31
	61.4	1.91	3.98	1.51	2.80
	66.4	1.65	2.53	1.09	2.24
	71.5	1.72	1.75	0.828	1.96
	76.5	1.85	1.42	0.820	1.74
	81.6	1.90	1.44	0.768	1.31
	86.6	1.74	1.49	0.609	0.949
	91.6	1.56	1.64	0.552	0.774
	96.6	1.36	1.61	0.536	0.658
	101.6	1.16	1.46	0.466	0.529
	106.5	1.05	1.19	0.424	0.606
	111.5	0.935	1.07	0.351	0.697
	116.4	0.935	0.99	0.322	0.835
	121.4	0.905	0.894	0.317	0.982
	126.3	0.916	0.894	0.309	1.06
	131.2	0.964	0.842	0.317	1.03
	136.1	0.886	0.915	0.374	0.966
	141.0	0.886	0.926	0.365	0.864
	145.9	0.838	0.894	0.313	0.617
	150.8	0.769	0.790	0.283	0.514
	155.7	0.672	0.728	0.219	0.401
	160.5	0.594	0.676	0.192	0.370
	165.4	0.526	0.645	0.166	0.396
	168.3	0.506	0.624	0.123	0.303
10.0	13.4	1.398	27.79	11.37	14.3
	15.4	1.445	27.52	9.92	12.9
	17.5	2.089	27.11	10.24	12.3
	20.5	2.486	23.71	7.54	11.4
	23.6	2.925	17.59	6.71	10.3
	26.7	3.948	11.67	4.45	8.03
	29.8	4.508	7.64	2.98	5.87
	32.8	4.857	4.73	1.83	4.38
	35.9	4.934	4.40	1.78	3.56
	39.0	4.552	4.65	1.59	3.07
	42.0	4.200	5.42	1.69	2.88
	45.1	3.441	5.06	1.76	
	48.1	2.887	5.07	2.61	3.46
	51.2	2.599	5.68	2.06	2.82
	54.2	2.184	5.34	1.73	2.57
	57.3	2.079	4.13	1.63	2.12
	60.3	1.813	3.04	1.05	1.85
	63.4	1.698	2.14	0.845	1.75
	66.4	1.744	1.94	0.728	1.62
	69.4	1.758	1.49	0.651	1.49
	72.5	1.875	1.21	0.552	1.40
	75.5	1.736	1.23	0.510	1.23
	78.5	1.746	1.25	0.505	1.12
	81.5	1.837	1.67	0.492	0.951
	84.5	1.637	1.67	0.529	0.842
	87.6	1.541	1.78	0.517	0.687
	91.6	1.375	1.70	0.479	0.626
	96.6	1.265	1.61	0.403	0.516
	101.5	1.013	1.42	0.332	0.482
	106.5	0.943	1.21	0.256	0.537
	111.5	0.930	0.964	0.295	0.584
	116.4	0.896	0.747	0.160	0.659
	121.4	0.938	0.723	0.386	0.778
	126.3	0.972	0.738	0.363	0.770
	131.2	0.982	0.686	0.336	0.747
	136.2	0.887	0.772	0.378	0.768
	141.1	0.796	0.816	0.424	0.759
	146.0	0.699	0.876	0.398	
	150.8	0.594	0.893	0.421	0.689

TABLE I (*continued*)

E_d (MeV)	$\theta_{c.m.}$	$\sigma(\theta)$ Q=6.14 MeV	4.19 MeV	3.67 MeV	2.19 MeV
10.0	155.7	0.518	0.744	0.438	0.906
	160.6	0.350	0.754	0.351	0.893
	165.4	0.301	0.534	0.206	0.691
	169.3	0.269	0.616	0.323	0.994
11.0	11.3	1.76	39.5	18.08	27.4
	13.4	1.87	40.8	18.34	24.5
	15.4	2.34	40.9	18.24	24.1
	17.5	2.84	38.5	15.73	22.9
	20.6	3.78	31.1	13.52	19.8
	23.7	4.85	22.7	10.71	15.8
	26.8	5.82	13.5	7.33	11.9
	29.8	6.58	8.37	3.90	6.47
	32.9	7.01	5.97	2.89	4.82
	36.0	7.23	5.30	2.77	3.55
	39.1	6.83	6.32	3.12	3.52
	42.1	6.02	6.94	3.17	3.55
	45.2	4.92	7.33	3.40	3.58
	48.3	4.08	7.13	2.98	3.27
	51.3	3.16	5.98	2.68	3.02
	54.4	2.67	4.58	1.89	2.19
	57.4	2.46	3.65	1.50	1.98
	60.5	2.24	2.69	0.989	1.83
	63.5	2.33	1.89	0.733	1.49
	66.6	2.45	1.52	0.693	1.27
	71.6	3.00	1.49	0.674	1.98
	76.7	2.82	1.86	1.07	2.16
	81.7	2.98	2.31	0.845	1.65
	86.7	2.04	1.72	0.754	1.19
	91.7	1.88	1.66	0.650	0.631
	96.7	1.63	1.26	0.491	0.377
	101.7	1.41	1.23	0.331	0.380
	106.7	1.34	1.14	0.228	0.441
	111.6	1.20	0.872	0.378	0.590
	116.6	1.26	0.848	0.463	0.707
	121.5	1.35	0.754	0.458	0.980
	126.4	1.32	0.754	0.359	0.938
	131.3	1.26	0.662	0.476	0.628
11.0	136.2	1.04	0.663	0.380	0.666
	141.1	1.06	0.697	0.434	0.472
	146.0	0.900	0.807		0.444
	150.9	0.709	0.761	0.355	
	155.7	0.551	0.796	0.322	
	160.6	0.428	0.701	0.326	0.285
	165.4	0.349	0.761	0.174	0.349
	169.8	0.338	0.569	0.141	0.476
12.0	10.3	1.05	29.0	12.3	6.84
	13.4	1.35	25.4	15.1	10.77
	16.5	1.91	29.5	13.6	15.35
	19.6	2.72	25.0	10.56	11.48
	22.6	3.69	18.6	7.95	9.09
	25.7	4.66	11.25	4.71	6.77
	28.8	5.49	6.88	2.00	5.10
	31.9	5.48	4.35	1.69	3.38
	34.9	5.57	4.20	1.63	2.84
	38.0	5.25	5.07	2.06	2.81
	41.1	4.08	6.01	2.21	2.93
	46.2	2.89	5.71	2.55	2.92
	51.3	2.13	4.38	1.38	1.88
	56.4	1.69	2.45	0.820	1.03
	61.5	1.72	1.44	0.510	0.942
	66.6	1.72	1.16	0.423	1.13
	71.6	1.85	1.17	0.510	1.19
	76.6	1.58	1.23	0.514	0.858
	81.7	1.49	1.14	0.451	0.606
	86.7	1.22	1.04	0.435	0.432
	91.7	1.05	0.894	0.330	0.242
	96.7	0.848	0.686	0.227	0.135
	101.7	0.749	0.686	0.239	0.161
	111.6	0.682	0.618	0.261	0.368
	121.5	0.709	0.479	0.235	0.448
	131.3	0.768	0.418	0.255	0.393
	141.1	0.562	0.485	0.253	0.271
	150.8	0.377	0.606	0.235	0.255
	160.6	0.216	0.516	0.184	0.242

[a] The standard deviations in the cross sections are believed to be ±10%.

While some of these fluctuations are probably due to nonuniformities in the Ca foil, some (especially at the lower energies) are certainly real fluctuations in the proton yield and contribute to the uncertainties in the DWBA analysis discussed later. It is interesting to note that, although the compound-nuclear contribution is probably greater at 90° than at 20°, the 20° fluctuations are qualitatively greater—in agreement with earlier measurements at much lower energy.[24]

The differential cross sections for the $Ca^{40}(d,p)Ca^{41}$ reaction to these four strong groups at the six deuteron energies used are listed in Table I. It is estimated that the over-all errors in these absolute cross sections are less than 10%, except for the back angles for the 3.95-MeV state as discussed above. Figures 4–7 show plots of these data and compared them with theoretical predictions calculated with the distorted-wave Born approximation as discussed below. In Fig. 8 the earlier data of Holt and Marsham[25] are compared with these same theoretical predictions. To obtain this good agreement with the predictions (and with our data), it is necessary to increase their absolute cross sections by 10%. This increase is within their estimated error of ±20%.

IV. COMPARISON OF EXPERIMENT WITH THEORY

First we specify the basic sets of parameters chosen for the calculations, and then we present detailed comparison of their predictions with the experimental data. In later sections we consider the effects of variations and uncertainties in those parameters.

A. Neutron Wave Function

The neutron is assumed to be captured into a shell-model orbit with orbital angular momentum l and total angular momentum $j=l\pm\frac{1}{2}$. This orbit we take to be an eigenstate in a potential well of Woods-Saxon shape, so that the wave function (and consequently the spectroscopic factor obtained upon comparison with experi-

[24] L. L. Lee, Jr., and J. P. Schiffer, Phys. Rev. **107**, 1340 (1957).
[25] J. R. Holt and T. N. Marsham, Proc. Phys. Soc. (London) **A66**, 565 (1953).

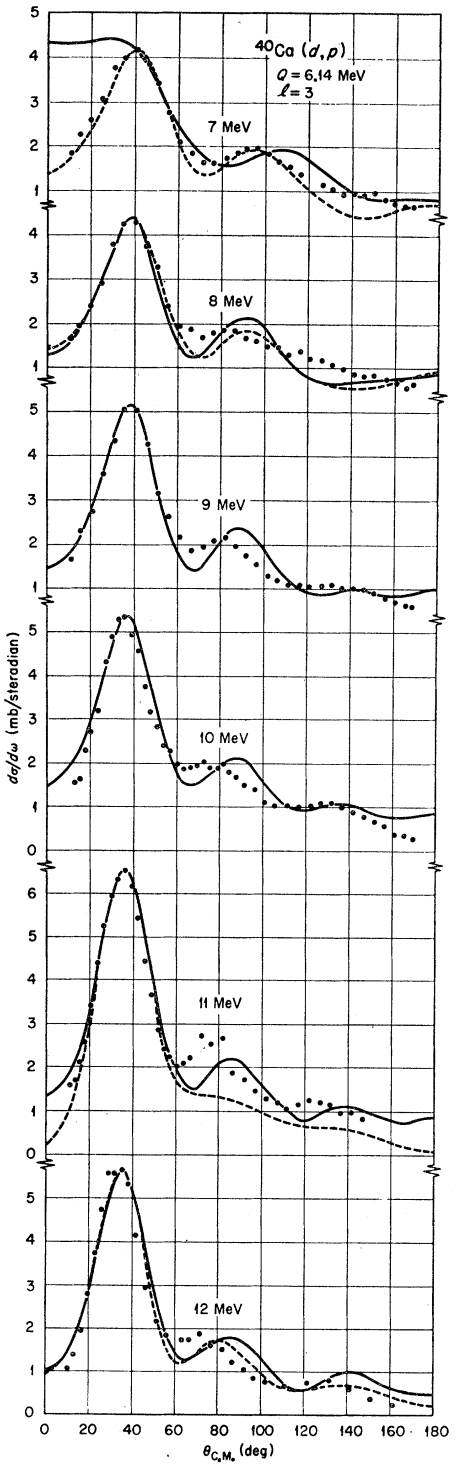

FIG. 4. Measured cross sections (dots) for $Q=6.14$ MeV at each deuteron energy. The full curves are theoretical predictions based on "best Z" potentials and zero-range approximation; spectroscopic factors are given in Table I. The dashed curve at 7 and 8 MeV uses "av. Z" potential and $S=0.93$ and 0.87, respectively. At 11 MeV, the dashed curve uses a cutoff at 4 F and $S=1.81$. The "best ZS" potential and finite range with spin-orbit coupling is used for the dashed curve at 12 MeV.

ment) is somewhat dependent upon the choice of parameters for this well, particularly upon the radius and spin-orbit coupling. In principle, this potential is obtained self-consistently in the Hartree-Fock sense, but in practice its parameters are not known too closely.

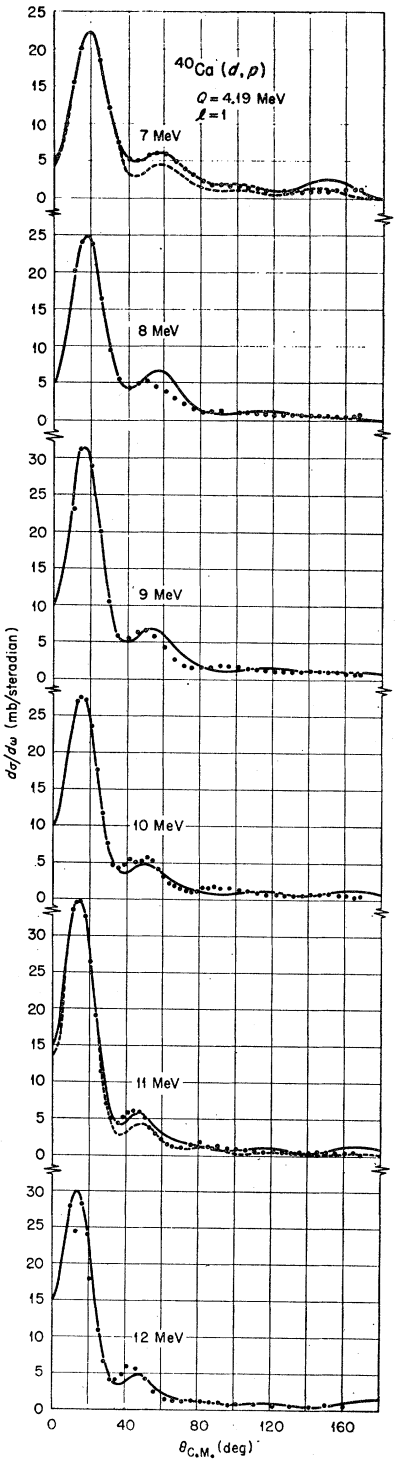

FIG. 5. Measured cross sections (dots) for $Q=4.19$ MeV at each deuteron energy. The full curves are theoretical predictions based on "best Z" potentials and zero-range approximation; spectroscopic factors are given in Table I. The dashed curves at 7 and 11 MeV use a cutoff at 4 F and $S=1.00$ and 0.78, respectively.

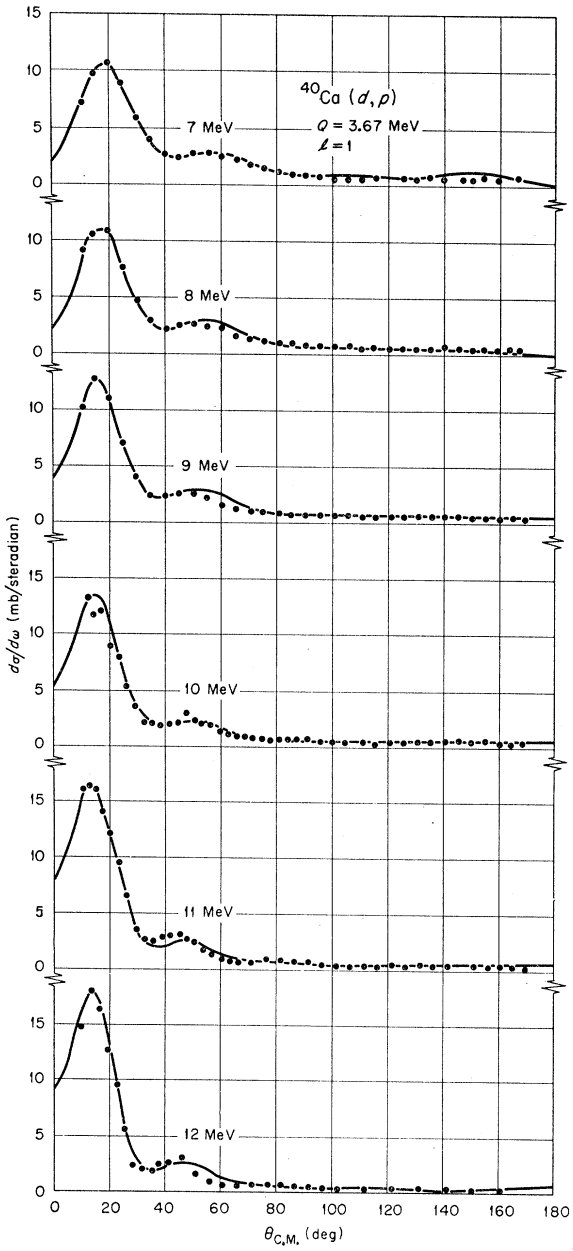

FIG. 6. Measured cross sections (dots) for $Q=3.67$ MeV at each deuteron energy. The full curves are theoretical predictions based on "best Z" potentials and zero-range approximation; spectroscopic factors are given in Table III.

For the calculations reported here, we assumed the same radius ($1.2A^{1/3}$ F) and diffuseness (0.65 F) as are used for the proton optical potential. When specified, a spin-orbit coupling 25 times the strength of the Thomas term was also included.[26] The depth of the well was adjusted to give a binding energy equal to the separation energy. When the spin-orbit coupling is included, the $1f_{7/2}$ ground state, with a separation energy of 8.37 MeV, requires a well depth of 56.4 MeV.

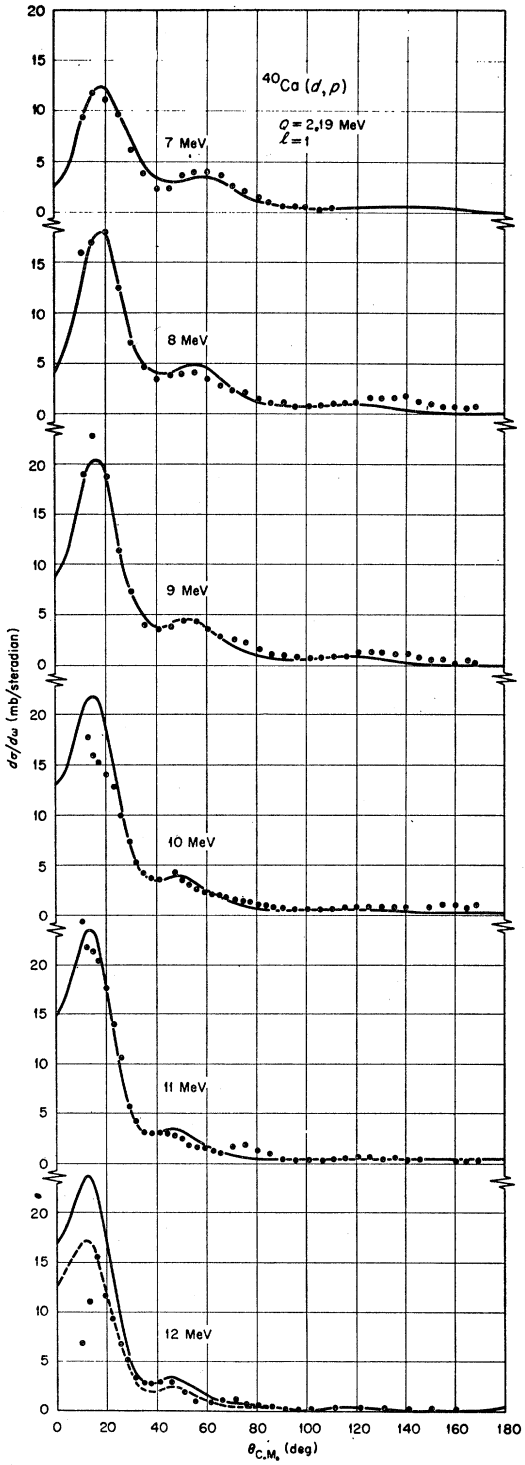

FIG. 7. Measured cross sections (dots) for $Q=2.19$ MeV at each deuteron energy. The full curves are theoretical predictions based on "best Z" potentials and zero-range approximation; spectroscopic factors are given in Table III. The dashed curve at 12 MeV uses $S=0.5$ instead.

[26] For the well depths needed here, this corresponds to a strength $V_s \approx 8$ MeV in Eq. (8).

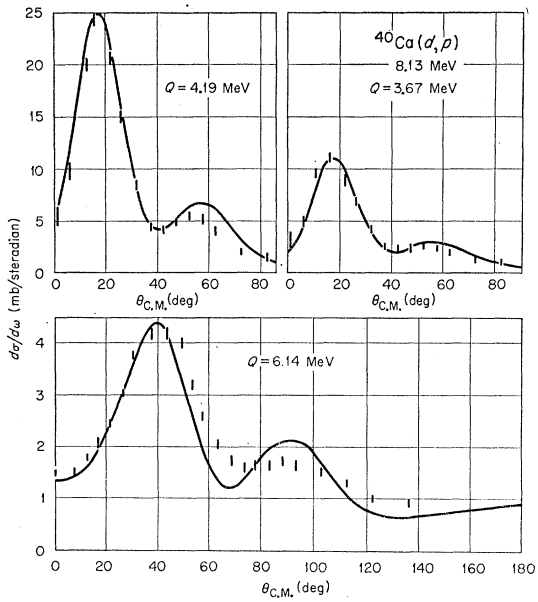

FIG. 8. Comparison between the data (points) of Holt and Marsham at 8.13 MeV and the predictions (curves) based on 8 MeV "best Z" potential and spectroscopic factors.

There are two candidates for the $2p_{3/2}$ state with energies of 6.42 and 5.90 MeV, which require well depths of 58.9 and 57.9 MeV, respectively. The $2p_{1/2}$ neutron is bound by 4.42 MeV which is obtained by using a well depth of 59.7 MeV. These well depths are in fairly close agreement, although there is no reason for them to be exactly the same.[27] (Somewhat better agreement would be obtained with a slightly weaker spin-orbit coupling, say 20 times the Thomas value.)

The radius $1.2A^{1/3}$ is probably close to a lower limit on the actual radius. An increase in this radius leads to an expansion of the bound wave functions, and hence to an increase in the predicted cross sections. An increase to $1.25A^{1/3}$ gives an increase of about 15% for the $l=3$ peak cross section, and about 10% for the $l=1$; the shapes of the angular distributions are unchanged. Thus, spectroscopic factors obtained from experiment on the assumption of a $1.2A^{1/3}$ radius are upper limits in this respect.

The cross section for capturing a neutron into an orbit with a given binding energy also depends upon whether or not spin-orbit coupling is used in calculating the wave function for that orbit. The peak cross section predicted for $1f_{7/2}$ capture, when the spin-orbit coupling is included in the neutron potential, is about 25% larger than when it is not, while for the $2p_{3/2}$ and $2p_{1/2}$ orbits the effect is about $\pm 5\%$, respectively. This result can be understood in the following way. Suppose we obtain an orbit with a certain binding energy in a spin-independent well. If we then switch on some spin-orbit coupling, the well depth has to be adjusted if we wish to keep the *same* binding energy. The well has to be made deeper if $j=l-\frac{1}{2}$, or shallower if $j=l+\frac{1}{2}$, in order to compensate for the repulsion or attraction, respectively, of the spin-orbit potential. However, since the spin-orbit coupling is a surface peaked potential, its effect on the *wave function* is more like that of an increase in radius for $l+\frac{1}{2}$ orbits, and a decrease for $l-\frac{1}{2}$ orbits. The wave function expands or contracts, and the cross section increases or decreases, correspondingly.

An alternative way of taking into account this spin-orbit effect in a spin-independent calculation would be to use an effective binding energy when constructing the neutron wave function (see Sec. V.A below). If, instead of using the actual separation energy S, one used a binding energy B which was greater than S if $j=l-\frac{1}{2}$, or smaller than S if $j=l+\frac{1}{2}$, a similar effect would be achieved. A suitable prescription might seem to be to use for the l orbit the binding corresponding to the center of gravity of the $l\pm\frac{1}{2}$ doublet. However, the figures quoted in Sec. V.A show that, while this prescription gives approximately the correct effect for the $1f$ orbit, it strongly overestimates it for the $2p$ orbit.

B. Proton Optical Potential

As remarked earlier, the proton potential used was based upon an analysis[13] of proton scattering from Ar^{40} in the energy range from 8 to 14 MeV. We adopted the surface-absorption form[12]

$$U(r)=U_c(r)-V(e^x+1)^{-1}+4iW_D(d/dx')(e^{x'}+1)^{-1}+(\hbar/m_\pi c)^2V_S\mathbf{L}\cdot\boldsymbol{\sigma}r^{-1}(d/dr)(e^x+1)^{-1}, \quad (8)$$

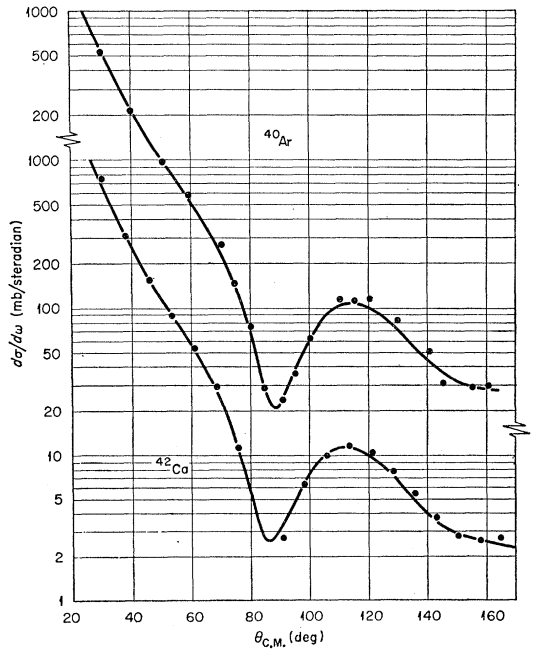

FIG. 9. Comparison between data for the elastic scattering of 12-MeV protons from Ar^{40} and Ca^{42} and predictions of the proton optical potential used in (d,p) calculations.

[27] K. A. Brueckner, A. M. Lockett, and M. Rotenberg, Phys. Rev. **121**, 255 (1961).

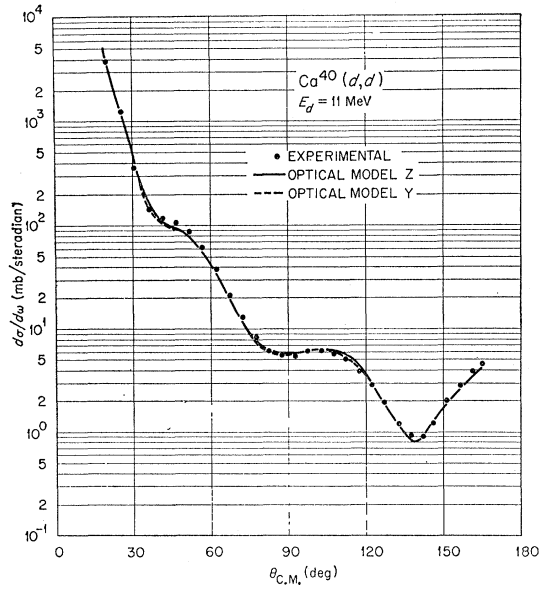

FIG. 10. Comparison between data for elastic scattering of 11-MeV deuterons from Ca^{40} and best-fit Y- and Z-type potentials (Ref. 11).

where

$$x=(r-r_0A^{1/3})/a, \quad x'=(r-r_0'A^{1/2})/a',$$

and U_c is the Coulomb potential from a uniform charge of radius $1.25A^{1/3}$ F. The values $r_0=1.20$ F, $a=0.65$ F, $r_0'=1.25$ F, and $a'=0.47$ F were found to give a good account of the Ar^{40} data, with a real well depth $V=(60-0.5E_p)$ MeV, absorptive strength $W_D=11$ MeV, and spin-orbit coupling $V_S=8$ MeV. The Ar^{40} data showed some preference for a real radius parameter $r_0=1.20$ F, contrary to the choice of Perey[12] who assigned the value 1.25 F to both radii. However, it is known that the elastic scattering is little affected by small changes in V and r_0, provided Vr_0^2 is kept constant, and with this rule there is close agreement between our choice and the recommendations of Perey. Further, it was verified by explicit calculation that the stripping cross sections remained unchanged when r_0 was changed to 1.25 F and Vr_0^2 kept constant.

A comparison between the predictions of this potential and the measured cross sections for 12-MeV protons on Ar^{40} are shown in Fig. 9, which also compares predictions with experiment for Ca^{42} at the same energy. These data were obtained after the present analysis was completed. Very satisfactory agreement is seen for both nuclides.

C. Deuteron Optical Potential

Several detailed analyses of deuteron elastic scattering have become available recently,[10] and have shown that there is considerable ambiguity in the choice of an optical potential. In particular, a whole series of potentials can be found which differ, crudely, only in the number of half-wavelengths which are included in the well.[28] The present measurement of the elastic scattering of deuterons from Ca^{40} was analyzed in a similar fashion; the results are presented in the preceding paper.[11] A potential of the form (8) was used. A set of potentials was found, with real well depths V ranging from 30 to 450 MeV in steps of about 40 MeV, which give practically identical scattering. Fits for two of these are shown in Fig. 10. No doubt even deeper potentials could be found. They do not predict the same stripping, however, for reasons which are evident from Fig. 11. This shows a cross section, taken along the incident direction through the center of the nucleus, of the distorted waves in the nuclear interior for the three shallowest potentials with real depths of about 30, 70, and 110 MeV. For even deeper potentials, the number of oscillations in the interior increases, and the focus moves closer to the center and becomes sharper. Beyond about 4 F, however, all the potentials (except X, the shallowest) generate closely the same wave function. Insofar as the region inside 4 F contributes significantly to the stripping reaction, these various potentials must predict different cross sections. This is illustrated in Fig. 12 for the $l=3$ ground-state group. This figure also shows that, except for X, the predictions become very similar when contributions from the region inside 4 F are eliminated, while with a cutoff at 5 F, X also predicts the same cross sections. Without a cutoff, we note that the deeper the potential, the smaller the predicted stripping cross section. Actually, potentials deeper than Z all give rise to stripping cross sections which are very similar to those obtained by use of a 4-F cutoff with the shallower potentials. This is readily understood; the rapid oscillations in the deuteron waves associated with these deep potentials almost completely eliminate the contributions that the stripping integrals receive from the nuclear interior.

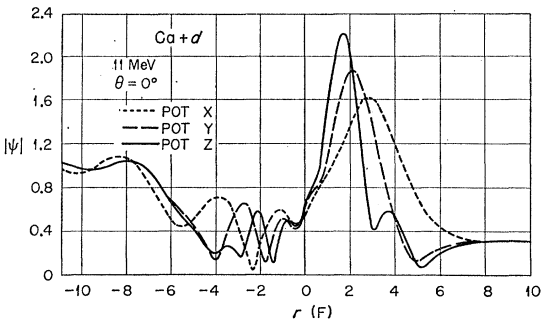

FIG. 11. Cross-sectional diagram of the distorted-wave deuteron wave functions in the nuclear interior, shown for three optical potentials giving the same scattering. This cross section was taken along the incident beam direction through the center of the nucleus. "Negative" radii refer to the illuminated side of the nucleus, positive radii to the shadow side.

[28] R. M. Drisko, G. R. Satchler, and R. H. Bassel, Phys. Letters 5, 347 (1963).

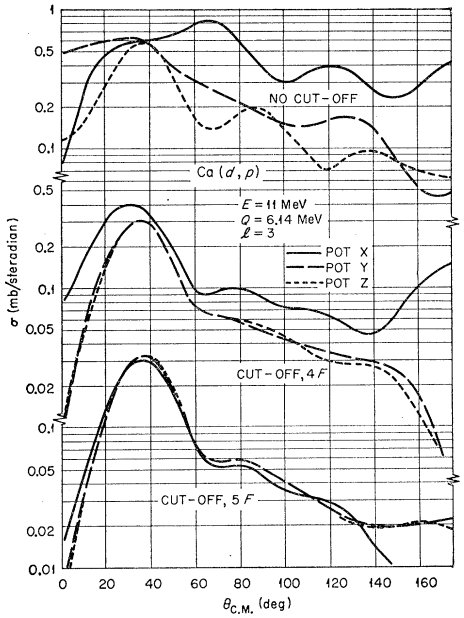

FIG. 12. Comparison of stripping predictions for the wave functions shown in Fig. 11.

Our first task then is to make some choice between these various deuteron potentials. If we believe this potential has any *physical* significance, we might expect it to resemble the sum of a neutron and proton optical potential, averaged over the internal motion of the deuteron. This would suggest a potential of depth about 100 MeV. Internal polarization of the deuteron ("stretching" and breakup), which is expected to be severe for such a loosely bound particle, would modify this estimate. However, it would be difficult to understand its leading to an effective potential much *deeper* than 100 MeV, although a shallower potential could not be ruled out on these grounds.

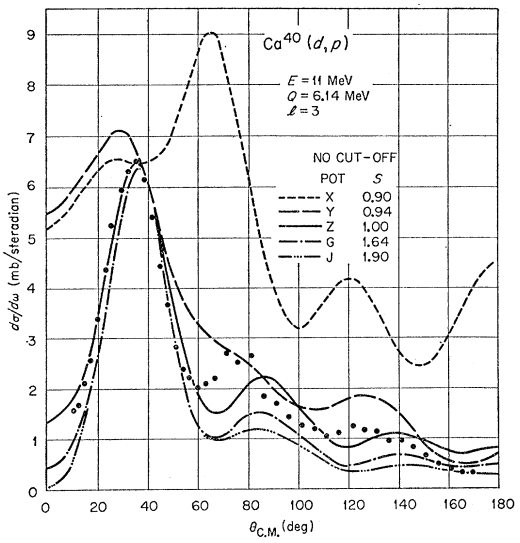

FIG. 13. Stripping predictions for $l=3$ with various potentials that give the same deuteron elastic scattering.

Aside from this prejudice, we may ask whether the experimental stripping data can distinguish between the various potentials. Figures 13 and 14 compare the predictions (in zero-range approximation) of some of these with the data at 11 MeV for $l=3$ stripping to the ground state and $l=1$ stripping to the first excited state of Ca^{41}. It is clear that the two shallowest potentials, X and Y, are unacceptable for both transitions. Potential Z gives a good account of the $l=1$ angular distribution. The $l=3$ group is not closely reproduced by any of the potentials, but the best fit is given by potential Z. Potentials deeper than Z (such as G and J shown in Figs. 13 and 14) predict similar stripping cross sections. The peak cross sections for $l=3$ are severely reduced (by almost a factor of 2), however, and the spectroscopic factors required to fit the measured cross section become considerably larger than unity. On the other hand, the $l=1$ cross section is little affected, so with these deeper

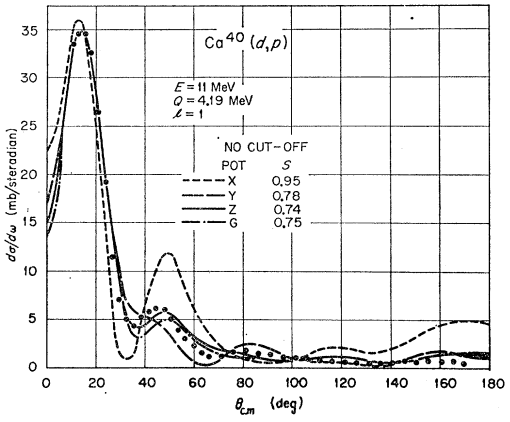

FIG. 14. Stripping predictions for $l=1$ with various potentials that give the same deuteron elastic scattering.

potentials we would be led to a surprising discrepancy between the $1f$ and $2p$ spectroscopic factors. Of course, since this investigation is intended to test the validity of the theory, these facts alone would not be sufficient grounds for rejecting the deeper potentials. However, in view of the prejudice against them discussed above, we feel justified in confining our attention to potentials of type Z. They give the best over-all fit to the data, and, as we shall see below, lead to a consistent set of spectroscopic factors.

Within this choice there are still ambiguities. In the preceding paper,[11] parameters were given for potentials of type Z which gave optimum fits to the elastic scattering at each energy. They were given both for no spin-orbit coupling ($V_S=0$) and for a fixed spin-orbit strength ($V_S=5$ MeV); these we shall refer to as the "best Z" and "best ZS" potentials, respectively. In addition, one of these given sets of parameters (with $V_S=0$) gave a reasonable fit to the elastic data at all

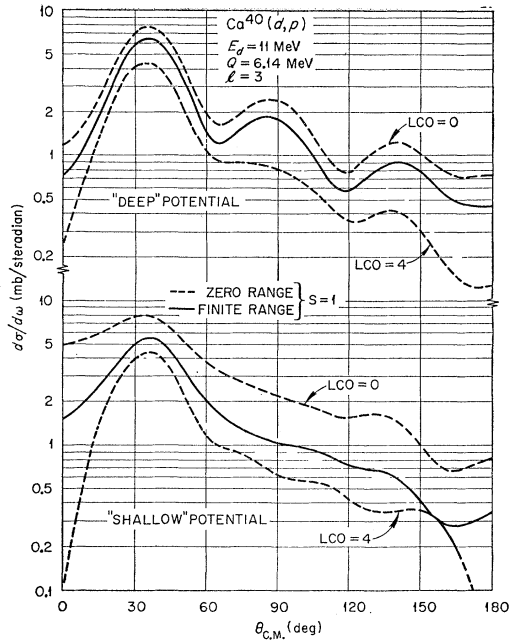

FIG. 15. Effect of finite range on the 6.14-MeV $l=3$ group. The "deep" potential is of type Z, the "shallow" of type Y. LCO denotes a lower cutoff on the radial integrations.

energies; this we call the "av Z" potential. The parameter values for this are $V=112$ MeV, $r_0=1.0$ F, $a=0.9$ F, $W_D=18$ MeV, $r_0'=1.55$ F, and $a'=0.47$ F.

Another ambiguity in the potential arises from the choice between volume or surface absorption. Experience has shown that potentials of either type can

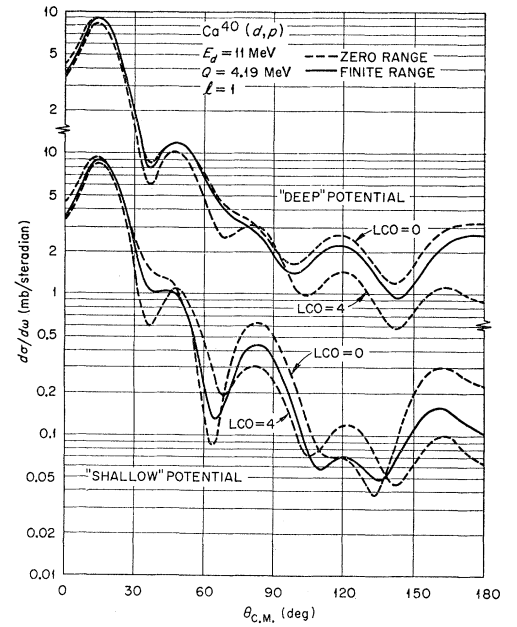

FIG. 16. Effect of finite range on the 4.19-MeV $l=1$ group. The "deep" potential is of type Z, the "shallow" of type Y. LCO denotes a lower cutoff on the radial integrations.

TABLE II. Variations of peak cross sections for a deuteron energy of about 11 MeV.

Effect	$1f_{7/2}$ $Q=6.14$ MeV	$2p_{3/2}$ $Q\approx4$ MeV	$2p_{1/2}$ $Q\approx2.19$ MeV
Finite range	−15%	+1%	+3%
Cutoff at 4 F	−45%	−6%	−6%
$B_{\text{eff}}=S\mp0.5$ MeV	±6%	±15%	±15%
Neutron spin-orbit, 8 MeV	+25%	+4%	−5%
Proton spin-orbit, 8 MeV	+5%	+3%	+1%
Deuteron spin-orbit, 5 MeV	−7%	−2%	+4%
Neutron radius 1.25 F	+15%	+10%	+10%

be found which give almost identical scattering.[10,11] Fortunately, as we shall see later (Fig. 24 below), this ambiguity has rather little effect on the stripping predictions.

D. Finite-Range and Radial Cutoff

Calculations were performed with the above potentials, both with the zero-range approximation and with a Gaussian finite-range function as in Eq. (7). The range 1.25 F was chosen to reproduce the low-momentum components of the Hulthén deuteron wave function. The effects of introducing finite range are shown in Figs. 15 and 16 for $l=1$ and $l=3$ transitions, both for a shallow (Y-type) and deep (Z-type) deuteron potential. As had been suggested,[17] one effect is to damp out the contributions from the nuclear interior; to emphasize this, curves are also shown for the zero-range cases in which a radial cutoff at 4F eliminates these contributions. The effect of both finite range and cutoff is greater for the "shallow" Y potential than for the deeper Z potential. The finite-range curves fall between those for zero range with and without cutoff. But the finite range by no means eliminates the interior contributions; rather, as we shall see later (Fig. 25 below), it reduces these contributions by about 30 or 40%. It should also be mentioned that if a radial cutoff is used in the finite-range calculation, it gives results almost identical to the zero-range approximation with cutoff. In other words, finite range has a negligible effect on the exterior contributions at these energies.

That the $l=1$ cross section is less sensitive to either finite range or a cutoff can be understood because the $2p$ wave function has a node in the interior. Its two parts of opposite sign then lead to cancellations which reduce the importance of the interior. Indeed, the partial damping of the interior which occurs when finite range is used actually gives a slight increase in the $l=1$ peak magnitudes (see Table II).

As discussed in the Introduction, it has been suggested[18] that there may be other reasons (such as doubts about the significance of the deuteron waves inside the nucleus) for eliminating the interior contributions by using a radial cutoff. One way of studying this question is by comparison with experiment. In the present case, we have seen (Figs. 12 and 15) that

TABLE III. Spectroscopic factors.

Q (MeV)	Quantity	Deuteron energy 7 MeV	8 MeV	9 MeV	10 MeV	11 MeV	12 MeV	Average
6.14	Peak (mb/sr)	4.2	4.4	5.15	5.37	6.55	5.65	
	S (av Z)[a]	0.928	0.866	0.925	0.894	0.943	0.876	0.91±0.03
	S (best Z)[a]	0.742	0.934	0.891	0.831	0.957	0.832	0.87±0.07
	S (best ZS)[b]	0.813	0.888	0.901	0.856	0.959	0.756	0.86±0.07
	S (av Z)[a,c]	1.54	1.52	1.70	1.68	1.99	1.63	1.67±0.16
4.19	Peak (mb/sr)	22.5	25.0	31.5	27.5	34.8	30.0	
	S (av Z)[a]	0.695	0.676	0.788	0.654	0.795	0.662	0.71±0.06
	S (best Z)[a]	0.843	0.745	0.830	0.676	0.713	0.566	0.73±0.09
	S (best ZS)[b]	0.891	0.732	0.840	0.532	0.664	0.536	0.72±0.12
3.67	Peak (mb/sr)	10.7	11.0	12.7	13.5	16.5	18.0	
	S (av Z)[a]	0.306	0.276	0.296	0.299	0.351	0.369	0.32±0.03
	S (best Z)[a]	0.375	0.301	0.316	0.307	0.319	0.320	0.32±0.02
	S (best ZS)[b]	0.394	0.299	0.316	0.289	0.294	0.299	0.32±0.04
	S (av Z)[a,c]	0.324	0.292	0.315	0.317	0.381	0.411	0.34±0.04
3.67+4.19	S (av Z)[a]	1.001	0.952	1.084	0.953	1.146	1.031	1.03±0.07
	S (best Z)[a]	1.218	1.046	1.146	0.983	1.032	0.886	1.05±0.10
	S (best ZS)[b]	1.285	1.031	1.156	0.921	0.958	0.835	1.03±0.15
2.19	Peak (mb/sr)	12.5	18.0	20.5	(21.9)	(23.5)	(24.0)	
	S (av Z)[a]	0.572	0.721	0.760	(0.77)	(0.81)	(0.78)	0.68±0.08
	S (best Z)[a]	0.691	0.784	0.820	(0.8)	(0.7)	(0.7)	0.77±0.05
	S (best ZS)[b]	0.732	0.779	0.838	(0.78)	(0.72)	(0.67)	0.78±0.04

[a] Zero-range approximation without spin-orbit coupling. [b] Finite-range approximation with spin-orbit coupling. [c] Radial cutoff at 4.1 F.

using a cutoff reduces the predicted peak cross section for the $l=3$ stripping by almost a factor of 2, whereas the $l=1$ cross section is little affected. We would then need $l=3$ spectroscopic factors larger than one, while the $l=1$ factors remain close to unity. So we conclude that using a cutoff cannot lead to a consistent set of spectroscopic factors, at least in this reaction. The evidence from the angular distributions is less clear. In some respects, the angular distribution *shapes* are improved qualitatively when a cutoff is used, although it also tends to predict too small a relative cross section at large angles. However, at this time, if the use of a cutoff does introduce some desirable features, we prefer to take this as an indication that our treatment of the interior contributions is not as good as it might be, rather than to use it to justify an arbitrary sharp cutoff. Hence, in the remainder of this work, we do not use a cutoff unless otherwise specified.

E. Compound-Nucleus Contributions

The contributions to the cross section from compound-nucleus processes were estimated by use of a form of the statistical model.[21] Because of the large number of open channels available, a level-density distribution has to be assumed for the residual nuclei. The channels included were elastic and inelastic scattering, and (d,p) and (d,n) reactions. Details of the calculations will be given elsewhere, but in summary the compound-nucleus contributions were found to be insignificant. For the ground-state (d,p) transition at 11 MeV, for example, the compound-nucleus cross section is estimated to be about 0.1 mb/sr at 0 and 180°, and about 0.05 mb/sr at 90°. At 8 MeV, these figures have increased to 0.14 and 0.11 mb/sr, respectively. Only at the largest angles do the observed cross sections approach these values. The compound-nucleus contributions to the $l=1$ transitions are even smaller. The estimated cross section for the $\frac{3}{2}^-$ state is about $\frac{1}{5}$ of that for the ground state, while for the $\frac{1}{2}^-$ it is about $\frac{1}{10}$ of the ground-state cross section. Only for deep minima such as that observed around 100° for the $Q=2.19$-MeV group, or at extreme back angles, would these cross sections be significant.

It should be remembered, however, that these are estimates of the energy-averaged cross sections. In the fluctuation region, with a resolution comparable to or better than the fluctuation length, interference between compound-nucleus and direct processes may produce considerably larger and energy-dependent contributions. There are some indications that the present experiment is approaching these conditions at the lower energies, but the effects seem to be sufficiently small that we do not need to consider them in detail.

F. Spectroscopic Factors

The solid curves shown in Figs. 4 through 7 were calculated in zero-range approximation and with complete neglect of spin-orbit coupling, by use of the "*best Z*" potentials. The spectroscopic factors S were adjusted to reproduce the estimated peak cross sections listed in Table III, where the S values are also given. The peak cross sections for the 2.19-MeV group at deuteron energies of 10, 11, and 12 MeV are difficult to estimate from the experimental results. In fact, they

were assumed to be given by the "*best Z*" predictions with spectroscopic factors of $S=0.8$, 0.7, and 0.7, respectively, values that give a reasonable over-all fit to the measured cross sections other than at the peak. Calculations were also made at each energy with zero-range and the "av Z" potential, and with finite-range and the "*best ZS*" potentials. For the latter, a spin-orbit coupling of 8 MeV was included for the proton and neutron. The group with $Q=6.14$ MeV was also calculated with finite range, the "av Z" potential, and no spin-orbit coupling. The corresponding spectroscopic factors are included in Table III. In addition, a large number of individual cases were calculated to test the effects of parameter variations; the results of some of these are reported below.

Before discussing these results, some attention should be drawn to the uncertainties and fluctuations associated with the experimental data. The excitation curves for the elastic scattering show some fluctuations with energy in the lower energy region, and this is reflected in the variations in the "best" optical-model parameters needed to fit the angular distributions.[11] The (d,p) cross sections also show some irregular variation with energy, an extreme example of which is shown in Fig. 17 where the changes between 11 and 12 MeV are compared with those expected theoretically. (See also the peak cross sections plotted in Fig. 18 below.) Another uncertainty arises from the difficulties experienced at 10, 11, and 12 MeV in determining the differential cross sections near the main peak for the group corresponding to $Q=2.19$ MeV.

The spectroscopic factors obtained from these analyses are summarized in Table III. The largest part of the errors (standard deviations) quoted for the average values of S arise from the uncertainties and fluctuations from energy to energy in the measured peak cross sections. These errors are larger for S values obtained with the "best" potentials. This reflects similar

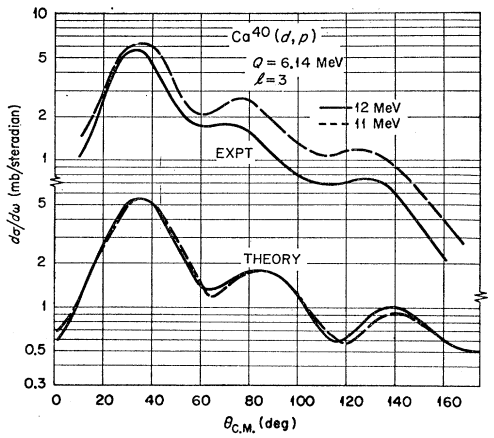

FIG. 17. Above: smooth curves drawn through the data taken at 11 and 12 MeV. Below: theoretical predictions at the same energies.

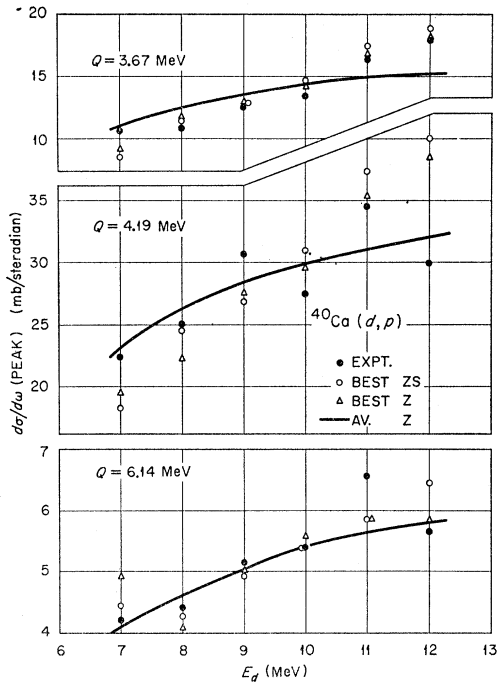

FIG. 18. Comparison between predicted and experimental peak cross sections as a function of energy. The predictions were based on the *average* spectroscopic factors from Table III.

variations in the measured elastic scattering and the corresponding best optical-model parameters. It emphasizes the possible dangers of placing too much weight on a measurement taken at a single energy, particularly for the lighter nuclei and at moderately low energies, unless one is sure that the energy dependence is very smooth in that region. It also emphasizes that the optical potential that gives the very best fit to scattering data at one energy is not *necessarily* the most physically significant one. Forcing the optical model in this way may bias the parameters unphysically because of errors or idiosyncracies in the data. An average fit to data at several close energies, or for neighboring nuclei, may be more significant in this respect. (A corollary to this is that the absence of elastic data in the exit channel at the appropriate energy, as in the present case, need not be a serious drawback, if data are available at similar energies for nearby nuclei.)

Another way of looking at these variations with energy is shown in Fig. 18, where the experimental and theoretical peak cross sections are plotted against energy. The theoretical values for each potential are normalized by use of the corresponding *average* spectroscopic factor from Table I. The fact that the "best" predictions show somewhat more fluctuation than the experimental values arises entirely from variations in the optical-model parameters. On the other hand, the calculations with the "av Z" potential vary smoothly with energy and give a good account of the average behavior of the cross sections.

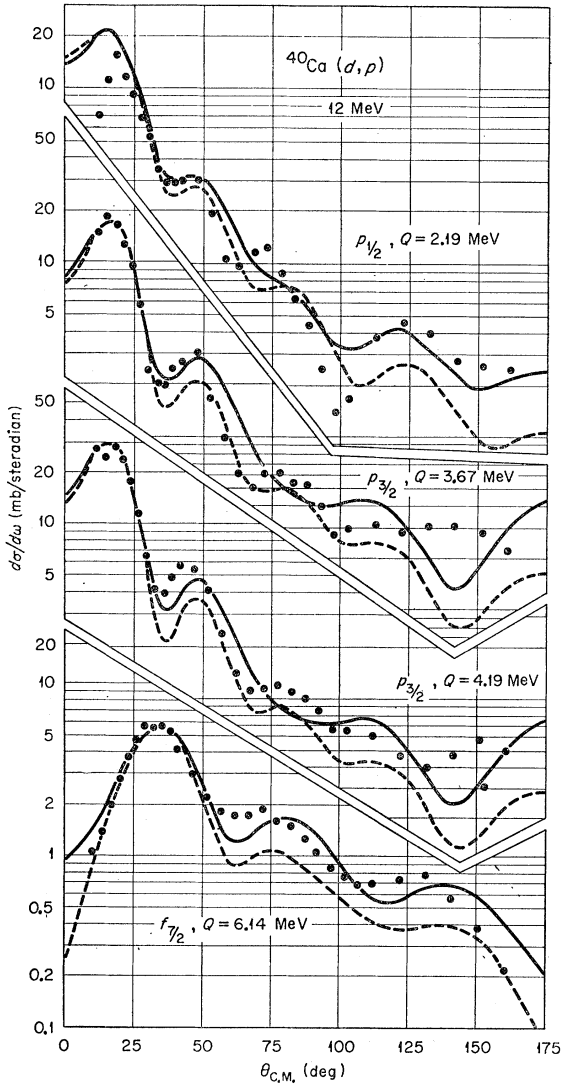

FIG. 19. Comparison between the experimental cross sections (dots) and the theoretical values based on the "best ZS" potential with finite-range and spin-orbit coupling. The full curves were computed without cutoff and with the spectroscopic factors from Table III. Dashed curves use a cutoff at 4 F and $S=1.10$, 0.58, 0.32, and 0.71 for the $Q=6.14$-, 4.19-, 3.67-, and 2.19-MeV groups, respectively.

The S values in Table III are close to the single-particle value $S=1$; in particular, the two $p_{3/2}$ levels together exhaust the $p_{3/2}$ strength. The $f_{7/2}$ and $p_{1/2}$ numbers are, perhaps, significantly less than unity; but in view of the remaining uncertainties in the analysis, it would be rash to speculate whether this really reflects a property of Ca^{41}. (One could anticipate, for example, that the $p_{1/2}$ single-particle character would be shared with one or more other states, just as is the $p_{3/2}$.) In any case, one can certainly say that the model for the reaction used here gives the expected results to better than 20%.

As shown by Figs. 4 through 7, the angular distributions are reproduced satisfactorily by the theory, especially for the $l=1$ transitions. On the other hand, there is evidence for some systematic deviations, in particular the second peak of the distributions for both $l=1$ and $l=3$ tends to be at larger angles than is seen experimentally. These discrepancies are not avoided by using finite-range or spin-orbit coupling. The logarithmic plots in Fig. 19 emphasize the smaller cross sections observed at large angles and show that the theory fits the data qualitatively over a range of two orders of magnitude. The theoretical curves were calculated by use of finite range and the "*best ZS*" potential, with spin-orbit coupling included for the neutron and proton. The dashed curves were evaluated with a radial cutoff at 4 F. To some degree, the cutoff results give the shapes of the large-angle distributions better; for example, they reproduce the shoulder near 70° for $l=1$. (The fits are improved if a larger value of the deuteron spin-orbit coupling is used.[29]) However, the *magnitudes* of the large-angle cross sections for these transitions are predicted too small, relative to the main peak, when a cutoff is used. In view of the remaining uncertainties both in the model parameters and in the experimental data, it does not seem wise at this stage to place too much emphasis on detailed fitting of these rather small cross sections. Nonetheless, it is gratifying that the model can reproduce the over-all features of the data to such an extent. It suggests that there is little room for introducing any additional transition amplitudes of appreciable magnitude.

G. J Dependence

It was recently pointed out[30] that this, and other (d,p) reactions in this mass region, show interesting systematic differences between the angular distributions at large angles for $p_{1/2}$ and $p_{3/2}$ capture. As we see from Fig. 19, the $p_{1/2}$ angular distribution shows a pronounced minimum at an angle of about 100°, in contrast to the $p_{3/2}$ groups. This behavior persists at all the energies studied here. It was also found in a variety of other (d,p) reactions, and has been used to identify the j value of the captured neutron.[30] Recent reports indicate that there is evidence for its appearance for other values of ^{31}l and in other direct reactions, such as (d,l) pickup.[32]

It is tautological to say this is a spin-orbit effect, since it is a difference between transitions in which neutrons are captured with $j=l\pm\frac{1}{2}$. However, it can be asked in which way spin-orbit coupling brings about this result, and whether the present theory is adequate to account for it. Figure 19 shows that the same qualita-

[29] G. R. Satchler, Argonne National Laboratory Report ANL-6878 (unpublished).
[30] L. L. Lee, Jr., and J. P. Schiffer, Phys. Rev. Letters **12**, 108 (1964).
[31] L. L. Lee, Jr., and J. P. Schiffer, Phys. Rev. **136**, B405 (1964).
[32] R. H. Fulmer and W. Daehnick, Phys. Rev. Letters (to be published).

tive behavior is produced by the calculations when spin-orbit coupling is included. The $p_{1/2}$ minimum is not as pronounced as that observed, and theory predicts a minimum at around 140° for the $p_{3/2}$ transitions, which is not seen experimentally. Both discrepancies are reduced when a larger value of spin-orbit coupling is used for the deuterons.[29]

Subsidiary calculations show that including spin-orbit coupling in the calculation of the neutron bound state has an indetectable effect on the angular distribution although, as discussed above, it does change the magnitude of the cross section by about 5%. However, including spin-orbit coupling in *either* distorted wave can be sufficient to produce effects of the order of those observed. It should be emphasized that the precise effect of spin-orbit coupling *in these calculations* does depend upon the values of the rest of the parameters being used. For example, Fig. 21, which is discussed in the next section, shows a case in which $p_{1/2}$ capture is predicted to have a weak minimum at about 100° in the absence of spin-orbit coupling, but to have *none* when proton spin-orbit coupling is included. These, and other results like them, lead us to believe that while the observed j dependence at back angles arises from the spin-orbit coupling in the proton and deuteron distorted waves, the remaining uncertainties in the theory do not allow us at this time to give a detailed account of the effect. Further studies are being made and will be reported elsewhere.

A qualitative explanation is easy to find. In the absence of spin-orbit coupling, the transition amplitudes linking the various magnetic substates of the spins in the entrance and exit channels are related to one another in a purely geometrical way, being weighted by the appropriate (real) Clebsch-Gordan angular-momentum coupling coefficients.[15] The introduction of spin-orbit coupling changes the weighting, and also the relative phasing, of these amplitudes. It is then quite

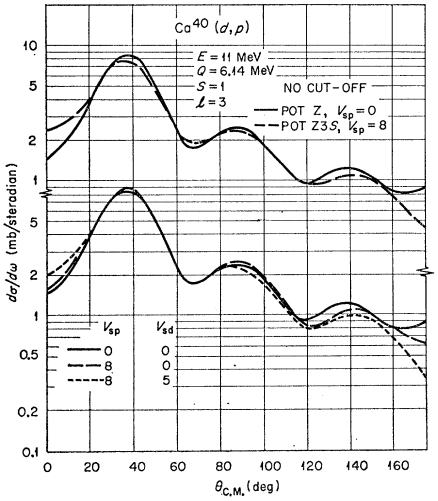

FIG. 20. Effect of spin-orbit coupling on an $l=3$ transition.

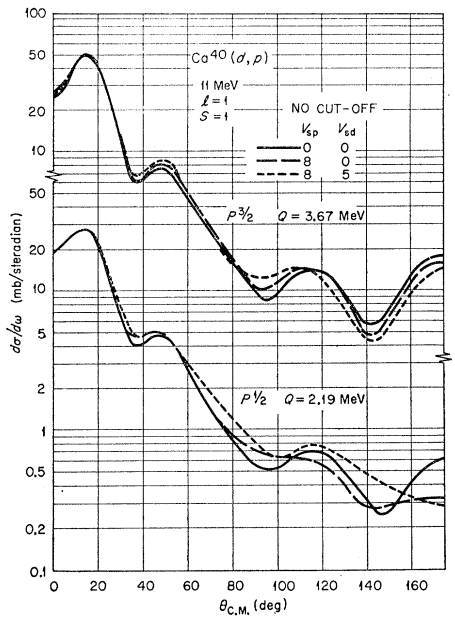

FIG. 21. Effect of spin-orbit coupling on an $l=1$ transition.

plausible that destructive interference between these amplitudes may occur at some scattering angle for one j value, but not for the other (for which the angular-momentum coupling is quite different). Indeed, if the spin-orbit coupling is weak enough for its influence on the distorted waves to be treated as a perturbation, the cross section may be written in the form[33]

$$d\sigma/d\omega \approx A(\theta) + (-1)^{j-l-\frac{1}{2}} B(\theta).$$

The term $A(\theta)$ is independent of the spin-orbit coupling, whereas $B(\theta)$ vanishes if there is no such coupling. This second term has opposite signs according as $j=l\pm\frac{1}{2}$. It may become comparable to the first term for large θ, and can produce the kind of cancellation needed. Because of the phase factor, cancellation for one j value implies reinforcement for the other.

It should also be noted that spin-orbit coupling produced no noticeable changes in the angular distributions near the main peak (see Figs. 20 and 21, for example), although Fig. 19 seems to imply that $p_{3/2}$ capture results in a marked minimum following the main peak, whereas $p_{1/2}$ capture does not. In fact, the differences seen in Fig. 19 arise solely from the different Q values and remain in the absence of spin-orbit coupling. The trend for the minimum to fill in as Q is reduced is already evident for the small change in Q between the 4.19- and 3.67-MeV groups.

H. Polarization Potential

The stretching of the deuteron by the Coulomb field of the nucleus can be partly accounted for by adding a polarization potential, proportional to r^{-4}, to the optical

[33] R. C. Johnson (private communication).

potential.[34] It has been shown[11] that this has a very small effect on the optical-model parameters for scattering of 7–12-MeV deuterons from Ca^{40}. Nonetheless, it might be thought that the cumulative effect of this long potential tail could significantly change the phases of the deuteron waves close to the nucleus, and hence modify the stripping predictions. However, the polarization potential was included in the distorted-wave calculations, and the results at 11 MeV were indistinguishable from those obtained without it. At 8 MeV, there are small differences in the optimum values of the optical parameters obtained by fitting the deuteron elastic data with and without the polarization term. These lead to small differences in the (d,p) predictions; the $l=3$ peak cross section is increased by 7% and the cross section at the 0° minimum is increased by 50%, when the potential with the polarization term is used. If, however, the polarization term is simply added to the "*best Z*" potential, the stripping peak is reduced 2%, and there is no other change.

An associated polarization effect is the spatial alignment of the deuteron as it approaches the nucleus. The neutron approaches more closely, on average, than the proton and, of course, it is this that gives rise to the polarization potential. Using the polarization potential reproduces the change induced in the motion of the deuteron center of mass, while the alignment represents a change in internal structure. Again, however, calculations have shown this to have quite small effects on stripping even from heavy nuclei at energies below the Coulomb barrier,[35] so we feel confident in neglecting it here.

V. VARIATIONS AND UNCERTAINTIES IN THE PARAMETERS

In this section we continue to discuss the effects on the distorted-wave calculations of variations and uncertainties in the various parameters. In particular, we deduce empirical corrections which can be applied to predicted peak cross sections in order to account for the effects of spin-orbit coupling and finite range. These are summarized in Table II. Although the discussion is based on the Ca^{40} (d,p) reaction, the results should be applicable to all such reactions at similar energies and on targets in this mass region.

A. Effective Binding Energy

The stripping amplitude (1) includes the overlap of the wave functions for the target and residual nucleus, integrated over the internal coordinates ξ of the target. The result,

$$\phi_{lm}(\mathbf{r}_n)=\int\psi_B^*(\mathbf{r}_n,\xi)\psi_A(\xi)d\xi,$$

is a function of the coordinates of the captured neutron. (For simplicity, we ignore the neutron spin and also assume that the target has zero spin so that ϕ has definite angular momentum.) We have no *a priori* knowledge of the function ϕ, although we like to think of it as proportional to a single-particle shell-model orbital, i.e., as an eigenstate of a nucleon moving in a central potential. We do know that asymptotically it has to behave like $[\exp(-Kr)]/r$, where K is the wave number corresponding to the actual separation energy S, the energy needed to separate the neutron from the product nucleus and leave the target nucleus in its ground state. It has been customary in calculations, as we have done here, to use for ϕ the wave function for a nucleon moving in a potential well adjusted to give a binding energy $B=S$. For a closed-shell target such as Ca^{40}, this is very reasonable, and only assumes that there is no appreciable rearrangement or readjustment of the Ca^{40} core when the extra neutron is added. For other nuclei, there is no real justification for representing ϕ in this way; even though it can always be expanded in the eigenstates of a potential well, there is no guarantee that one such term will give an adequate representation. One might argue that, in the spirit of the shell model, ϕ is proportional to the *zero-order* single-particle orbital that would be used in a shell-model calculation before the residual interactions were switched on. It would then be calculated in the same way, but with an "effective" binding energy $B_{\text{eff}}\neq S$. There is some experimental evidence in favor of this procedure.[29,36] (The extreme tail of ϕ then has an incorrect form, but we have to assume that this introduces negligible errors.) In general, the larger B_{eff}, the smaller the predicted cross sections. The reduction comes partly from the more rapid falloff of ϕ outside the nucleus, partly from the over-all contraction of the wave function. For binding energies of around 6 MeV in this mass region, a change of 0.5 MeV in B_{eff} produces roughly a 15% change in peak cross section for $l=1$, and about 6% for $l=3$.

This effect could arise to a small extent for the two $p_{3/2}$ transitions in $Ca^{40}(d,p)$, if we assume that the *same* neutron wave function should be used for both. A calculation for the $Q=3.67$-MeV groups was made with $B_{\text{eff}}=6.42$ MeV, which is the separation energy associated with the other group ($Q=4.19$ MeV). The peak cross section is 15% less than that obtained with the separation energy, 5.90 MeV. The reduction decreases slowly with increasing angle, until in the backward direction the cross section is unchanged. Otherwise, the angular distribution is unaffected.

The use of a fixed bound-state wave function, independent of variation in separation energy, could strongly affect our measure of the spectroscopic factors for small

[34] C. F. Clement, Phys. Rev. **128**, 2728 (1962).
[35] A. K. Kerman and F. P. Gibson, Argonne National Laboratory Report ANL-6848, p. 43 (unpublished).
[36] J. L. Yntema, Phys. Rev. **131**, 811 (1963); B. Zeidman (unpublished); R. Sherr, E. Rost, and B. Bayman, Bull. Am. Phys. Soc. **9**, 458 (1964); R. Sherr, E. Rost, and M. E. Rickey, Phys. Letters **12**, 420 (1962).

fragments of the single-particle strength which may be found in levels at higher excitation. Consequently, it also would strongly affect our measure of the energy-weighted moments of the spectroscopic factors. The justification for this prescription is purely empirical[29,36] at present; further theoretical work is necessary before it can be said to be understood.

B. Neutron Bound State

The previous section raised the question whether one could satisfactorily represent the overlap function $\phi(\mathbf{r}_n)$ by an eigenstate of motion in a one-body potential well. In general, the answer to this question is not known, but we have explored a little the consequences of varying the shape of ϕ.

The effects of varying the radius and spin-orbit strength when ϕ is calculated with a Woods-Saxon potential have already been discussed in Sec. IV.A. An alternative prescription for ϕ that has been used[6,7] takes an harmonic oscillator function (with the appropriate l and principal quantum number n) which is matched to a Hankel function $h_l^{(1)}(iKr)$ at some radius R_N. This has the correct asymptotic form if K is the wave number given by the neutron separation energy. Experience has shown that for $n=1$ and 2 (as is the case in Ca^{41}), it is always possible to choose R_N so as to closely reproduce in this way the ϕ calculated by use of a Woods-Saxon potential and the same binding energy. As the number of nodes n increases, it becomes increasingly difficult to match the ϕ calculated in these two ways. Because the oscillator potential lacks the central flat portion of the Woods-Saxon potential, the amplitudes of the oscillations in its eigenfunction near the origin are always larger. However, the $1f$ and $2p$ wave functions (with spin-orbit separation) used in the calculations reported here are closely reproduced by using a value[37] $R_N=5.2$ F, and the stripping predictions with these modified oscillator functions are almost unchanged. On the other hand, if the Hankel function with its exponential tail $\propto[\exp(-Kr)]/r$ is replaced by the Gaussian tail of the oscillator function, the result is a drastic reduction in the stripping cross sections, and some change in the angular distribution. The $l=3$ peak cross section is reduced by a factor of 2, the peak is broadened, and the whole distribution is shifted by about 5° toward larger angles. (This last effect can be interpreted as a reduction in the effective interaction radius due to the shorter tail of the oscillator function.)

C. Spin-Orbit Coupling

We have already discussed the j dependence of angular distributions which can be produced by spin-orbit coupling. We continue the discussion of spin-orbit coupling here, with emphasis on changes in the magnitudes of the cross sections. For most purposes, spin-orbit coupling has a negligible effect on the shapes of angular distributions, unless one is concerned with small changes such as the $p_{1/2}-p_{3/2}$ differences discussed above. This is illustrated in Figs. 20 and 21, where proton and deuteron spin-orbit terms are simply added to a zero-range calculation using the "av Z" potential. As previously remarked, this particular calculation does *not* reproduce the observed $p_{1/2}-p_{3/2}$ difference at back angles. Figure 20 also shows a comparison between the spin-independent "best Z" deuteron potential, and a similarly optimized potential $Z3S$ which did include spin-orbit coupling.[11] (Potential $Z3S$ has $V_s=4.74$ MeV, and otherwise differs from Z mainly in having a weaker imaginary part.) Most of these shape differences would be invisible in a linear plot of the curves; but the spin coupling does have important consequences for the peak magnitudes, and hence for the spectroscopic factors extracted by comparison with experiment. This is emphasized in Fig. 22, where linear plots for the $l=3$ peak are presented for various spin-orbit combinations, all normalized to $S=1$ and calculated with the Z deuteron potential. The curve labeled Z includes no spin-orbit coupling, while $Z+N$ includes it for the neutron bound state. As already remarked, this "expands" the wave function for $j=l+\frac{1}{2}$, and in this case the cross section is increased by 24%. An added 8 MeV of proton spin-orbit interaction (curve $Z+NP$) further increases the cross section so that it is 30% larger than for the Z curve. Further, adding a 5-MeV spin-orbit term for the deuterons ($Z+NPD$) brings it down again to only 21% larger than for the spinless case Z.

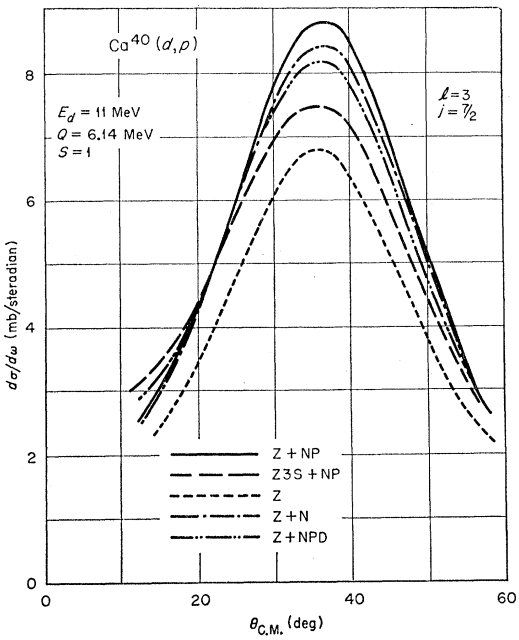

FIG. 22. Effect of spin-orbit coupling on an $l=3$ peak cross section.

[37] It should be noted that the value of R_N required is considerably larger than the radius $1.2A^{1/3}=4.1$ F of the Woods-Saxon potential.

Because the deuteron spin-orbit strength is relatively unknown at the present time, the comparison of cases ($Z+NP$) and ($Z3S+NP$) is of interest. Both include 8 MeV of spin coupling for the neutron and proton; the true value is known to be close to this. Then these two cases represent the best we can do when we use best fits to the elastic deuteron scattering without and with spin-orbit coupling, respectively. We see that there is an 18% difference. This arises mainly because, when we include spin-orbit coupling in the optical-model analysis, we have to readjust the other parameters (especially the absorptive strength W_D) to regain a good fit to the elastic data.[11] A similar comparison at a deuteron energy of 12 MeV leads to a similar effect—but of opposite sign. This partly reflects variations in the elastic data, but also the difficulty of determining the spin-orbit strength from analysis of differential cross sections alone. At 12 MeV, the optimum strength is $V_s=8.2$ MeV and the associated absorptive potential is reduced by about $\frac{1}{3}$. (This also re-emphasizes the possible dangers of relying too heavily on the use of absolute best-fit parameters in a reaction calculation.) Polarization measurements on the elastic scattering would be necessary to determine V_s more precisely. At the present time we see that, at a given energy, there is an error of some 20% associated with the peak cross section in this energy region because of the uncertainty. At the lower energies, spin-orbit coupling has considerably less effect on the elastic scattering, and its inclusion in the distorted waves has less effect on the stripping predictions, so that this uncertainty is reduced.

D. Variations in the Optical Potential

The optical-model parameter in which there is greatest uncertainty is probably the strength of the absorptive potential. Figure 23 shows how the differential cross sections vary when W_D for the deuterons is varied by 25%. The peak cross sections vary roughly as W_D^{-1} for $l=3$, and as $W_D^{-1/2}$ for $l=1$. The $l=3$ transition is more sensitive because it receives larger contributions from the nuclear interior than does the $l=1$. (Compare, for example, the effect of a cutoff as shown in Figs. 15 and 16.) The effect of W_D becomes more pronounced as the angle increases, but the variation is smooth, so the over-all shape of the angular distribution is little changed. Varying W_D for the protons has a very similar, but smaller, effect; halving W_D only increases the $l=3$ peak by 20%.

There is a possible argument for using a smaller value of W_D for deuterons in the stripping calculation than is required to fit the elastic-scattering data. Part of the absorption corresponds to deuteron breakup, but this part of the wave function can still contribute to the (d,p) reaction through the consequent capture of the neutron and escape of the proton. If this can be accounted for approximately by reducing the value of W_D used in the stripping calculation, the results just cited show that the major effect would be a simple increase in the cross section.

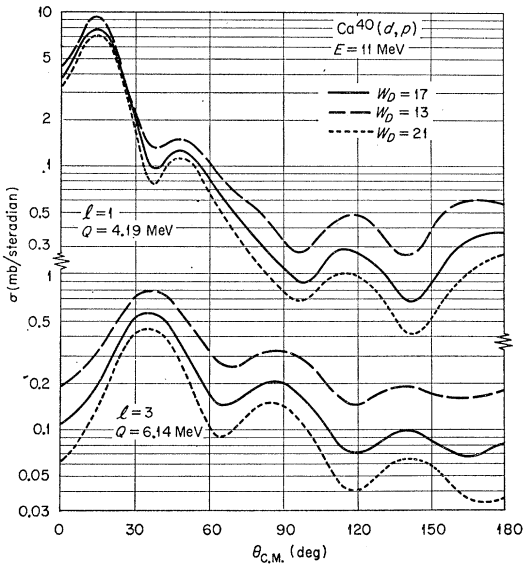

FIG. 23. Effect of varying the deuteron absorptive potential for a Z-type potential.

Another uncertainty associated with the absorptive potential concerns its radial distribution. It is known that for deuterons,[10,11] and to a lesser extent protons,[12] equally good fits to elastic-scattering data can be obtained with either volume or surface absorption. Fortunately, this ambiguity is of little consequence for deuteron stripping at these energies, as illustrated in Fig. 24 for the type-Z deuteron potentials.

A further ambiguity with the proton potential is that the predicted scattering is practically unchanged by small changes in V and r_0 that keep the product Vr_0^n constant, where $n\approx 2$. Calculations were made with r_0 increased to 1.25 but with Vr_0^2 kept constant, and the changes in the stripping cross sections were negligible.

E. Interior Damping

The effects of eliminating the contributions to the stripping amplitude from the nuclear interior by using a radial cutoff have already been discussed. For whatever reasons one might wish to reduce these contributions, a more physically reasonable procedure could be a smooth, partial cutoff such as is illustrated in Fig. 25. There the contribution from the interior is damped by 50%, with a smooth transition to no damping across the nuclear surface. The values of the cross section fall between those with and without a sharp cutoff, but the shape of the angular distribution remains close to that for no cutoff. Referring back to Fig. 15, we see indeed that introducing a finite range is equivalent to approximately a 30–40% reduction in these contributions from

the interior. The $l=1$ transition is affected in much the same way.

It was pointed out in Sec. II that if the optical potentials used to generate the distorted waves and the neutron bound state were nonlocal, the corresponding wave functions inside the potential well would be smaller than those generated by local potentials.[20] Since three of these functions appear in the stripping amplitude, a 15–20% reduction in each would greatly reduce the importance of the nuclear interior; the damping would approach that used in Fig. 25. However, the normalization of the neutron wave function must be conserved; any reduction in magnitude inside the nucleus must be compensated by an increase in the magnitude of the tail. The stripping cross section is roughly proportional to the square of the normalization factor of the neutron tail (it would be exactly so if the contributions from the interior were absent); in the present case, this increase roughly cancels the decrease due to interior damping.

Approximation techniques are being used to study nonlocal effects in stripping, and the results will be reported elsewhere.[38] For our present purpose, we take the view that we are investigating the usefulness of the local theory, and will not consider nonlocal effects further.

F. Summary

A summary of some of the effects we have discussed is presented in Table II, which lists the approximate changes in peak cross section. These results are based upon zero-range calculations using the Z-type deuteron potential at deuteron energies of about 11 MeV. The numbers are only intended to be a rough guide, since

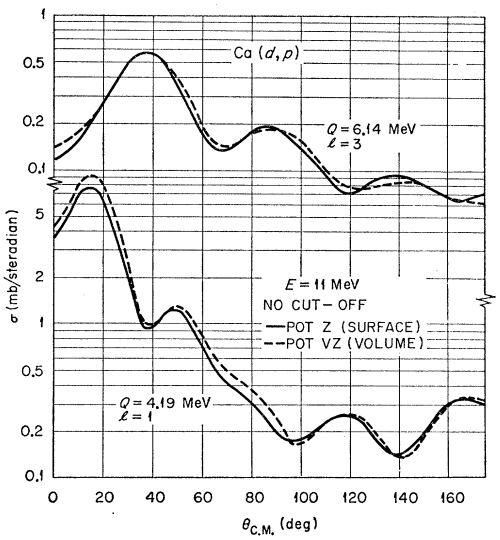

FIG. 24. Comparison of stripping predictions based on deuteron potentials with volume (dashed curves) and surface (solid curves) absorption which give the same elastic scattering.

[38] F. G. Perey (private communication).

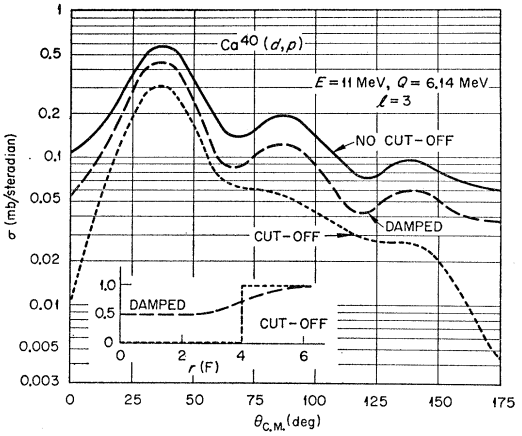

FIG. 25. Effect on $l=3$ stripping of smoothly damping interior contributions by 50% compared to use of a sharp cutoff. The "av Z" deuteron potential was used.

their precise values depend upon all the other parameters. In addition, we would estimate a possible error of up to 20% due to the over-all uncertainties in the deuteron optical potential. Uncertainties in the proton potential usually have much less effect on the stripping.

The *relative* magnitudes of peak cross sections, for different groups or different l values, are less subject to these uncertainties (except for such special effects as the j dependence introduced by spin-orbit coupling), so that relative spectroscopic factors should be somewhat more reliable than their absolute values.

VI. EXTRAPOLATED POTENTIALS

It often happens that elastic-scattering data are not available for the same nucleus or the same energy as the reaction data. So it is relevant at this point to enquire about the consequences of using some average set of deuteron optical parameters deduced from scattering on nuclei from another region of the periodic table, or based upon qualitative analyses with a simplified potential. As an example of the first type, we may use the Set-B parameters suggested for heavier nuclei by Perey and Perey,[10] while for the second we may take the Woods-Saxon potential recommended by Hodgson.[39] The elastic scattering predicted by these gives a poor fit to that measured (Fig. 26). The reason[10,11] for this is that the data require the imaginary potential to extend to considerably larger radii than the real potential. Ca^{40} is not exceptional in this respect; it is a general trend exhibited by the lighter nuclei.

In Fig. 27, the result of using these potentials in a stripping calculation is compared with the result obtained with the "best Z." The over-all fit to the data is not bad, although the $l=3$ peak is shifted a few degrees with Hodgson's potential, and the $l=3$ intensity away

[39] P. E. Hodgson, in *Proceedings of the Conference on Direct Interactions and Nuclear Reaction Mechanisms, Padua, 1962*, edited by E. Clementel and C. Villi (Gordon and Breach Science Publishers, Inc., New York, 1963).

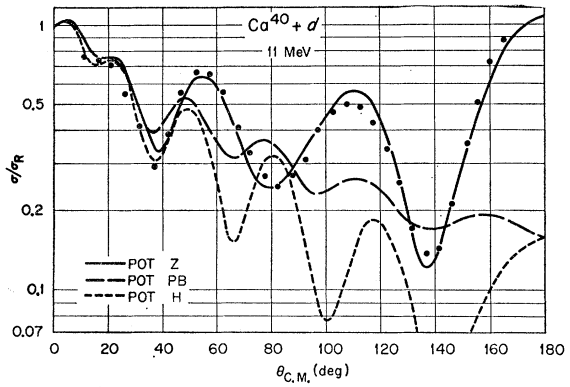

FIG. 26. Comparison between the measured cross sections (dots) and three theoretical predictions (curves) of deuteron elastic scattering. The predictions are based on the potential (*H*) of Hodgson, the set-B potential (*PB*) of Perey and Perey, and the "best *Z*" parameters.

from the main peak is seriously underestimated by the Pereys' potential. The characteristic discrepancy in the position of the second $l=3$ peak is reproduced by all three potentials.

Other calculations, not shown, indicate that these two potentials also reproduce reasonably well (to about 10–20%) the variation of peak cross section with energy

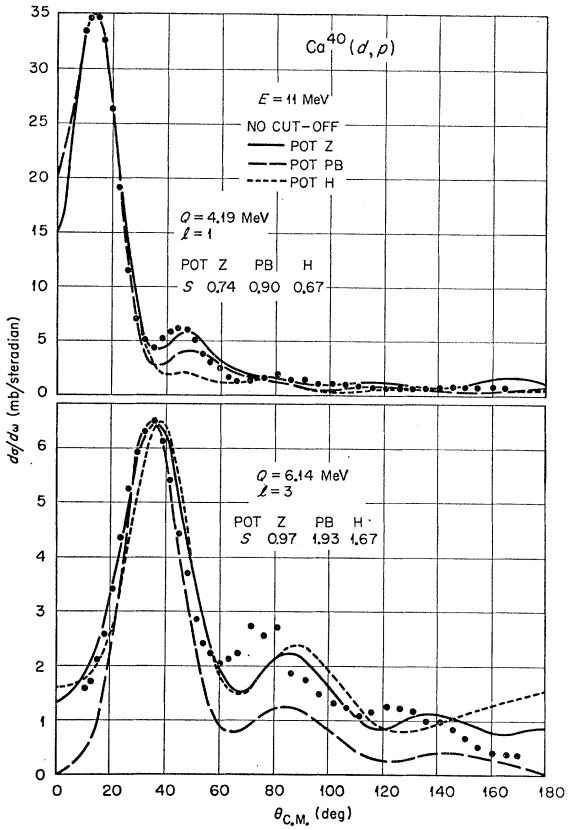

FIG. 27. Stripping predictions based on the same deuteron potentials as for Fig. 26.

and *Q* value. However, the absolute magnitudes (and hence the spectroscopic factors) are in serious error. In particular, the ratio of $l=1$ to $l=3$ peak intensity is in error by almost a factor of 2 with both potentials when compared to the "best *Z*" ratio.

We conclude that *reasonable* guesses at the potentials will probably fit the main peak of the angular distribution (*without* adjustable parameters), and will predict energy and *Q* dependence with fair accuracy; but they may be in serious error (that is, by factors of the order of 2) for both absolute magnitudes and relative magnitudes for different *l* captures. To ensure more reliable predictions, we need to have more knowledge of the behavior of optical-model parameters in the mass region being studied. It is safe to interpolate, but may not be safe to extrapolate.

VII. DISCUSSION

The purpose of the present work was to discover how reliably differential cross sections for deuteron stripping could be predicted by use of the distorted-wave method and that part of the amplitude (1) due to the V_{pn} interaction. The $Ca^{40}(d,p)$ reaction was chosen because there are reasons for expecting it to exhibit spectroscopic factors of unity, at least for the ground-state transition.[40] This expectation was borne out to within 20%, so that we believe this version of the theory is capable of making predictions to this accuracy.

It must be said that this is probably better than we had a right to expect, in view of the discussion of Sec. II. Indeed, the success of the one term considered here further enhances the need for reliable estimates of the other contributions to the amplitude [for example, from the bracketed interactions in Eq. (2)]. Such calculations have been started, and the results will be presented in due course.

Many of the deviations between experiment and theory are no larger than the differences between the experimental cross sections at different energies, or the variations which can arise from small changes in the theoretical parameters. However, there are some significant discrepancies, e.g., the inaccuracy in reproducing the second peak of the $l=3$ angular distributions. Further, it is not yet clear that the *j* dependence of the $p_{1/2}$ and $p_{3/2}$ angular distributions can be completely

[40] Further work on the reaction at 7 MeV [T. A. Belote (private communication)] has shown three other $l=1$ transitions, feeding levels at 3.62, 4.61, and 4.76 MeV. They require values of $(2j+1)S(p_j)$ of approximately 0.20, 0.20, and 0.40, respectively, if we use the av *Z* deuteron potential and put the neutron's binding energy equal to its separation energy. If, for example, we assume all three are $\frac{1}{2}^-$ levels, the total $p_{1/2}$ strength observed would become approximately 1.08 ± 0.08, close to the summed $p_{3/2}$ strength (Table I). An $l=3$ transition to a level at 4.89 MeV is also observed; under the same conditions it requires $(2j+1)S(f_j)=0.63$. This is only one-tenth of the single-particle strength, so this level cannot be the $1f_{5/2}$ single-particle state. It may represent a fragment of it, or of the $1f_{7/2}$ state. If the latter, it would bring the total $1f_{7/2}$ strength observed to 0.99 ± 0.03. It becomes of considerable interest to determine the spins of these levels in order to test these assumptions.

accounted for by the present form of the theory. The fits to data for heavier nuclei (for example,[41] on Zr^{90}) are often considerably better than those exhibited here. This is presumably because at least some of the additional contributions to the stripping amplitude neglected here become less important as the target nucleus becomes heavier. Exchange contributions exhibit this behavior. One might also expect more complete cancellation between the neglected interactions of Eq. (2).

Although the details of the predicted differential cross sections are sensitive to the precise values of the parameters of the model, the over-all features (such as the position of the main peak, or the decrease in cross section as the angle increases) show considerably less sensitivity. Reproduction of these features requires only the correct selection of angular momenta[42] (localization in angular-momentum space); this is ensured by the strong-absorption properties of deuteron scattering. (To this must also be attributed the successes of the diffraction, or strong-absorption, models.[43]) These aspects of the reaction and its *spatial* localization will be discussed in more detail in a later paper.

The differential cross section is not the only quantity which may be compared with experiments; measurements are also available on the proton polarization[44] and the p-γ angular correlation[45] for the $Ca^{40}(d,p)$ reaction in this energy region. The predictions of the theory for these quantities will also be discussed elsewhere.

ACKNOWLEDGMENTS

The authors are indebted to Dr. F. Perey and Dr. R. C. Johnson for helpful discussions, to E. Kowalski and J. McShane for their help in taking the data, and to the Argonne tandem operating group. We also wish to thank Frank Karasek for fabricating the thin Ca foils, and F. Taraba for programming the data reduction.

[41] W. R. Smith, Argonne National Laboratory Report ANL-6848, p. 30 (unpublished); J. K. Dickens and F. G. Perey (to be published).

[42] N. Austern, in *Proceedings of the Rutherford Jubilee International Conference, Manchester 1961*, edited by J. B. Birks (Heywood and Company, Ltd., London, 1962); and in *Selected Topics in Nuclear Theory*, edited by F. Janouch (International Atomic Energy Agency, Vienna, 1963); E. Rost, Phys. Rev. **128**, 2708 (1962).

[43] A. Dar, Phys. Letters **7**, 339 (1963); E. M. Henley and D. V. L. Yu, Phys. Rev. **133**, B1445 (1964).

[44] M. Takeda, *Proceedings of the International Conference on Nuclear Structure, Kingston, Canada, 1960*, edited by D. A. Bromley and E. W. Vogt (University of Toronto Press, Toronto, 1960); W. P. Johnson and D. W. Miller, Phys. Rev. **124**, 1190 (1961); R. W. Bercaw and F. B. Shull, *ibid.* **133**, B632 (1964).

[45] R. Taylor, Phys. Rev. **113**, 1293 (1959); L. L. Lee, Jr., J. P. Schiffer, and D. S. Gemmell, Phys. Rev. Letters **10**, 496 (1963).